

# We are IntechOpen, the world's leading publisher of Open Access books Built by scientists, for scientists

**4,800**

Open access books available

**122,000**

International authors and editors

**135M**

Downloads

Our authors are among the

**154**

Countries delivered to

**TOP 1%**

most cited scientists

**12.2%**

Contributors from top 500 universities



**WEB OF SCIENCE™**

Selection of our books indexed in the Book Citation Index  
in Web of Science™ Core Collection (BKCI)

Interested in publishing with us?  
Contact [book.department@intechopen.com](mailto:book.department@intechopen.com)

Numbers displayed above are based on latest data collected.

For more information visit [www.intechopen.com](http://www.intechopen.com)



---

# Uniform EPR Spectra Analysis of Spin-Labeled Macromolecules by Temperature and Viscosity Dependences

---

Yaroslav Tkachev and Vladimir Timofeev

Additional information is available at the end of the chapter

<http://dx.doi.org/10.5772/45931>

---

## 1. Introduction

Spin labeling method crossed its 47-th anniversary. It was invented in 1965 by Harden McConnell. He was the first who reported EPR spectra of bovine serum albumin and poly-(L-lysine) with stable nitroxide radicals chemically bound, and attempted to interpret them (Stone et al., 1965). As it stands today, we must conclude that there is little consensus between different scientists on the problem of such EPR spectra interpretation. When stepped into area of studying much more sophisticated biological objects comparing to these McConnell used, spin labeling methods this problem appeared to be very difficult. Its difficulty arises not only from the objects complexity, but also from method limitations, which relies on the solution of EPR reverse problem. Even with all of extensive developments done since 1965, such as availability of new microwave frequencies and pulsed EPR techniques, which, in fact, grew into separate method, the problem remains. It originates from large discrepancy between the information content of EPR spectrum and underlying object's behavior. Systems studies modern life science is interested in displays such a large degree of versatility that simply does not fit into single spectrum. This work summarizes our attempts to address this issue during the past 30 years.

The key for interpreting EPR spectra uniquely is to use as much of experimental data as possible. The most of informational content is found in spectra containing broad outer peaks (BOPs), as otherwise strongly narrowed spectra are highly degenerate, and attempting to solve reverse problem from them with underlying model which is slightly more complex than trivial is prone to non-uniqueness. Our method is primarily based on spectra with BOPs, to extract the most of useful information. In spectra of liquid solutions, their position is strongly affected by the mobility of nitroxide, and it is modulated by nitroxide

environment and macromolecule Brownian motion. These are two main contributions into EPR lineshape the method is capable to resolve with most objects being studied.

We have previously suggested that monitoring the position of the broad outer peaks (BOPs) in EPR spectra of spin-labeled macromolecules unravels the system dynamics to the maximum extent conventional EPR can deliver. This may be achieved by studying of so-called temperature and viscosity dependencies, or TVDs, for short. In many cases, they provide a key to the interpretation of EPR spectra of spin-labeled macromolecules, by eliminating the large degree of non-uniqueness arising from different kinds of molecular motion. Similar approach is applicable to the non-covalent spin probe EPR studies of membranes. From these dependencies one can experimentally determine two very important quantities: the rotational correlation time ( $\tau$ ) of the protein molecule, and McConnell's order parameter ( $S$ ) of rapid spin-label motion. Possibility of immediate use of these parameters for computational simulation of the EPR spectra significantly contributes to unique interpretation.

McConnell pioneered the use of the BOPs position in EPR spectra depending on the value of correlation time of a nitroxide radical motion. He conducted theoretical (McCalley et al., 1972), using Bloch equation, and experimental (Shimshick & McConnell, 1972) studies of the spin labeled alpha-chymotrypsin. Kuznetsov (Kuznetsov et al., 1971) theoretically showed the dependence of low-field BOP shift on the value of nitroxide molecular motion correlation time. J. Freed (Goldman et al., 1972) theoretically derived the expression for separation between BOPs depending on the value of  $\tau$  for nitroxide radical.

We in parallel worked with the same problem, but for some reasons our first work has been published only in 1977 (Dudich et al., 1977). In this work it was emphasized for the first time that it is necessary to consider partial averaging of nitroxide magnetic tensors due to the fast reorientation of spin label relative to the macromolecule. This fast motion effectively changes the values of nitroxide magnetic tensors components. Most of the studies mentioned above were focusing on influence of polarity of an immediate NO $\cdot$  moiety environment. Although this influence is not challenged, the polarity effects from nearby amino acid residues are very object-specific, as the surface charge of protein is. It is also pH-dependent, making it very difficult to follow. Additionally, in many practical cases the nitroxide moiety of attached label is significantly exposed to solvent, reducing polarity change effects. The fast motion is still ubiquitous, as neither label-to-protein linkage, nor the local protein structure at labeling site is perfectly rigid. In J. Freed's work (Mason and Freed, 1974) this fast motion relative to the carrier (molecular unit label is bound to) was considered as very rapid motion with respect to one of the molecular axes, while setting the diffusion tensor components in perpendicular plane to very slow motion, with an artificial introduction of tilt between the diffusion tensor principal axes relative to magnetic tensors ones.

The method based on averaging and is similar to known Model Free (MF) approach widely accepted in NMR (Lipari and Szabo, 1982). In this method, fast motion is considered to be independent of overall tumbling. The complicated Slowly Relaxing Local Structure (SRLS) model developed by Freed (Meirovitch et al., 2007) is claimed to benefit from including the

coupling between these motions. It is achieved by substitution of composite diffusion operator into stochastic Liouville equation. This point was recently shown to be challengeable (Halle B., 2009). With simplified two-dimensional SRLS model Halle showed that attempting to exploit an advantage over MF it takes from motions coupling, lead to rather unphysical conditions. The contention was that complication introduced in SRLS probably does not worth its theoretical benefits.

Here we will present a clear algorithm suitable for correct and unequivocal interpretation of EPR spectra according to two independent motions (TwIM) model. As an example we will present an EPR study of spin-labeled Barstar in solution as well as attached to sepharose adsorbent to eliminate slow tumbling. Parameters measured from temperature and viscosity dependencies will be fed into the EPR spectra simulation program, and resulting spectra compared to experimental ones. We also show how the given approach may be naturally extended to membrane structures. Joint use of this method, together with Molecular Dynamics simulations, allows deeper investigation of the object's nature.

## 2. The temperature and viscosity dependence of EPR spectra of spin-labeled macromolecules

As it was noted in Introduction, an informational content of single EPR spectrum is rather limited. A case when both slow tumbling and fast label motions are indistinguishable from single lineshape is frequently encountered. The method of temperature and viscosity dependences (TVD) is found extremely helpful here, although other approaches also exist (e.g., multifrequency EPR, where the relative sensitivity to motions on different time scales at various radiofrequency bands is utilized to resolve them). The TVD method developed throughout many years in a close connection with progress in computer hardware and software technologies. At present time, it can be utilized for unambiguous simulation of EPR spectra of spin-labeled macromolecules (Dudich et al., 1977; Timofeev, 1986, 1993, 1995) with easily available equipment (X-band spectrometer and personal computer) and minimum effort. The main idea this method is based on is pretty straightforward, once the TwIM model is assumed. In this model, the overall motion of spin label is composed of two independent components, one related to rapid motion of nitroxide-containing molecular fragment, and another to entire macromolecule tumbling. The former usually have correlation times in order of 100 ps or less, and, therefore, is *fast* on timescale of EPR method at X-Band. If this motion would be perfectly isotropic, its main effect is limited to some Lorentzian line broadening. In spin labeling applications, however, this is not usually the case, as the object (typically protein) spin label is attached to, significantly hinders nitroxide mobility. This is regarded as *motion anisotropy* in TwIM model, and it is quantified by order parameters. Its effect is much stronger: it changes the position of resonances, and this shift has severe impact on EPR spectrum. Effective spin Hamiltonian partial averaging is an efficient method to account for these changes. In fact, the only change in simple nitroxide spin Hamiltonian is different values of magnetic tensor  $g$  and hyperfine tensor  $A$ . This partial tensor averaging technique was utilized for studying anisotropic phases since early

history of the spin labeling. Macromolecule tumbling correlation times lie typically in nanosecond range. The anisotropy of this motion is generally determined by the shape of macromolecule in liquid solution, and for most globular proteins the single isotropic “effective” correlation time ( $\tau$ ) is sufficient to describe the lineshape change induced by it. At X-Band, presumed here if no otherwise stated, and nitroxide spin labels, the  $\tau$  values in range of 1-100 ns leads to significant changes in lineshape, which may be calculated by means of stochastic Liouville equation (SLE).

Henceforth we assume that the main EPR-observable effect of fast nitroxide fragment motion is changes in its *anisotropy*, quantified by order parameter  $S$ . For the slow tumbling, the corresponding quantity is its correlation time  $\tau$ . This anisotropy-correlation time splitting presumed in TwIM model allows to eliminate much of the ambiguity from EPR spectra interpretation. But even in this case it may be very difficult to distinguishingly quantify the effects of both contributions from single lineshape. This is where temperature-viscosity dependence comes into play. Varying sample temperature, one can modulate both kinds of motion:  $\tau$  decreases with temperature, and order parameter  $S$  typically do so due to increasing of molecular motion amplitudes. The viscosity of solution (which is also dependent on temperature), can be independently varied by addition of sucrose, glycerol or some polymer media. It mainly affects the correlation time  $\tau$ , while interference with small-scale fast molecular motions is typically observed only at very high viscosity, where it is, strictly speaking, not “fast” anymore. In the TVD experiment, the set of EPR spectra is recorded, at different temperatures and solution viscosities. The processing of resulting dependence starts with analysis of separation between broad outer peaks in spectrum, according to the procedure described below.

## 2.1. The theory of temperature-viscosity dependences

The method of temperature and viscosity dependence was originally proposed (Timofeev & Samarianov, 1995) to determine the correlation time  $\tau$  of slow isotropic rotational diffusion of a macromolecule, and McConnell’s order parameter  $S$  in axially symmetric case. This method was further developed and modified (Tkachev, 2010) to be suitable for smooth joining into spectra interpretation and simulation framework based on TwIM model. The primary quantity measured experimentally in this method is the separation between the broad outer peaks (BOPs) in X-Band conventional EPR spectra (absorption spectra derivative). Independence of slow Brownian diffusion of entire macromolecule treated as rigid entity, and fast anisotropic reorientations of spin label, as the basic concept of TwIM, is the fundamental proposition in TVD method. Both motion types narrow the lineshape, shrinking the separation between BOPs (referenced as  $2A'$  here). If one considers fast motion by anisotropic (partial) averaging of effective spin Hamiltonian, the amount  $2A'$  decreases will depend on motion ordering, or, speaking other way, its degree of anisotropy. The slow tumbling, which in many cases of globular proteins can be thought isotropic, lead to the same effect but now it is dependent on the correlation time. This means one can express an effective shift of BOPs as the sum of the shifts originating from these two motion components:

$$2A_{ZZ} - 2A' = (2A_{ZZ} - 2\bar{A}) + (2\bar{A} - 2A') = \Delta_1 + \Delta_2 \quad (1)$$

where  $2A_{ZZ}$  – the separation between BOPs in rigid-limit EPR (“powder”) spectrum. It was originally found from experiment, that plotting the  $2A'$  value versus the temperature and viscosity ratio  $\eta$ , yields linear dependencies at constant temperature. The point where the extrapolated line crosses the ordinate axis yields the  $2\bar{A}$  value. In approximation of axial symmetry of the fast motion, it is possible to derive dependence of the first term  $\Delta_1$ , on McConnell’s order parameter  $S$ :

$$S = \frac{2\bar{A}_{11} - 2\bar{A}}{2A_{zz} - 2A} = \frac{2\bar{A} - 2a_0}{2A_{zz} - 2a_0} \quad (2)$$

where  $a_0 = (A_{XX} + A_{YY} + A_{ZZ})/3$  is the isotropic hyperfine splitting constant of nitroxide radical. Therefore, the value of  $\Delta_1$  is represented as:

$$\Delta_1 = 2A_{ZZ} - 2\bar{A} = (2A_{ZZ} - 2a_0)(1 - S) \quad (3)$$

The second term  $\Delta_2$  gives the shift of BOPs in relative to the  $2\bar{A}$  value. The value of  $\Delta_2 = 2\bar{A} - 2A'$  can be evaluated in the following way. Spectral lineshape narrowing due to an exchange (Slichter, 1981), caused by slow rotation of a macromolecule with correlation time  $\tau$ , is defined by the following expression ( $\gamma$  is a magnetogyric ratio):

$$\Delta H' \approx \Delta H \left[ 1 - \left( \frac{2}{\gamma\tau\Delta H} \right)^2 \right] \quad (4)$$

In the model of an exchange between two states we assume them to be parallel and perpendicular orientations relative to magnetic field (Z axis). Corresponding values of  $\Delta H$  and  $\Delta H'$  will be

$$\Delta H = 2(\bar{A}_{11} - \bar{A}) = 3(\bar{A}_{11} - a_0) = 3S(A_{ZZ} - a_0) \quad (5)$$

$$\Delta H' = 2(A'_{11} - A') = 3(A'_{11} - a_0) \quad (6)$$

Using expressions (2, 5, 6), we write  $\Delta H'$  as follows:

$$\Delta H' = 2(A'_{11} - A') = \Delta H - \frac{3}{2}\Delta_2 \quad (7)$$

Now, combining (7) with the expressions (4, 5) we finally obtain

$$\tau S = \frac{1}{3\gamma\Delta_0} \left( \frac{\Delta_2}{\Delta_0 S} \right)^{-\frac{1}{2}}, \quad (8)$$

where  $\Delta_0 = 2(A_{ZZ} - a_0)$ .

Hence, the dependence between the BOP shift, correlation time  $\tau$  of a macromolecule tumbling, and order parameter  $S$  of fast spin label motion, should be found in the following form:

$$\tau S = a \left( \frac{\Delta_2}{\Delta_0 S} \right)^{-b} \quad (9)$$

Empirical parameters  $a$  and  $b$  can be found from a set of simulated EPR spectra at various values of  $S$  and  $\tau$ . The formula (9) is deduced in the dimensionless form, therefore parameter  $a$  has the dimension of nanoseconds. Parameters  $a$  and  $b$  are dependent on changes of initial magnetic tensors and individual line width. But their mutual dependence (they always derived simultaneously, and are not independent) makes splitting (1) weakly affected by these changes. For the most of experiments with spin-labeled samples the value of  $a$  is close to 1.1 ns, and parameter  $b \approx 1.3$ .

To establish a link with experimentally measurable values – temperature  $T$  and viscosity of a solution  $\eta$ , the straightforward way is to call for Stokes-Einstein relation (describing rotational motion of a sphere in a viscous media):

$$\tau = \frac{V\eta}{kT} \quad (10)$$

In this case expression (9) takes a form:

$$\Delta_2 = \Delta_0 S \left( \frac{akT}{SV\eta} \right)^{\frac{1}{b}} \Leftrightarrow 2A' = 2\bar{A} - \Delta_0 S \left( \frac{akT}{SV\eta} \right)^{\frac{1}{b}} \quad (11)$$

The overall result here is that the separation between BOPs is a linear function of  $\left( T / \eta \right)^{\frac{1}{b}}$ . Experimental measurement of this dependence by varying the temperature and the viscosity, it is possible to find  $2\bar{A}$ , and corresponding order parameter  $S$ , and, according to the formula (9), rotational correlation time of a macromolecule tumbling in solution. It's important to remember, however, that derived expressions are valid only when motions differ significantly on time scale. This may not be the case at very high viscosities where shear forces may interfere with the fast motion, which is believed to be affected solely by temperature changes. At these conditions motion of nitroxide cannot be regarded as 'fast' anymore.

## 2.2. The uniform method for resolving an EPR spectroscopy reverse problem

Combining the EPR spectra simulation using TwIM model for motion of spin label, and experimental approach of TVD, the following scheme can be used for uniform spectra interpretation. It allows unequivocally treat the line shape modulated by different dynamic effects. It calls for stochastic Liouville equation approach for calculation of slow motional EPR spectra. The flowchart is shown on Fig. 1, and individual steps are described in the following sub-sections. It contains two feed-back optimization cycles: one on the right relies on TVD data (experimental), but it corresponds to axially symmetrical case. The one on the

left is more general, and deals with rhombic components of magnetic tensors (more than one order parameter is possible to describe fast motion). Right cycle **1** is responsible for locking the BOP separation in simulated spectra to experimental values, and for distinguishing between fast and slow motional contribution to BOP shift (ca. expression (1)). The generalized cycle **2** allows obtaining finer details of the motion (additional order parameters) from fitting the XY manifold (central region of EPR spectrum). The procedure is considered complete when both cycles are consistent.

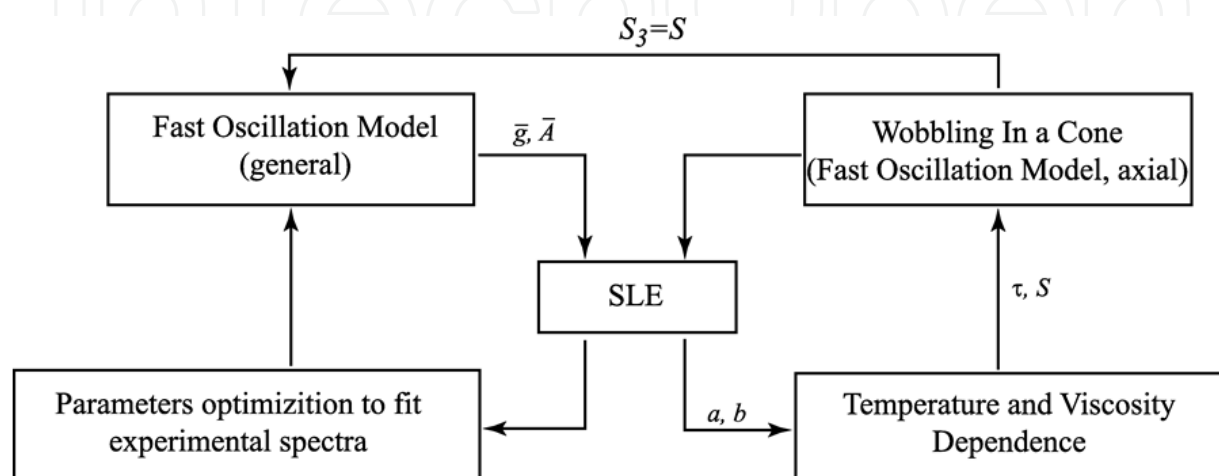


**Figure 1.** The scheme of uniform EPR spectra interpretation based on TwIM model and TVD experiment. SLE states for stochastic Liouville equation-based procedure for calculation of slow motional spectra.

### 2.2.1. Determination of magnetic tensors components

The entire procedure was designed to eliminate as many degrees of freedom as possible while retaining physical sense. The lineshape changes induced by molecular motions are controlled via  $\tau$  and  $S$ . To set up spectra simulation, magnetic parameters have to be determined in some way. Blind fitting of them would scramble all the averaging effects, and therefore is not suitable here. The most correct way is using diluted crystal, but its production in many cases is not feasible. The compromise is to use values of  $2a_0$  from free label solution EPR spectrum at room temperature and  $2A_{ZZ}$  from spectrum of frozen labeled sample at 77K. The rhombic component still remains unknown, and has to be fitted. For hyperfine A tensor, it is small, and the values of  $A_X$  and  $A_Y$  are almost equal. This mostly eliminates the A-tensor problem, which is mostly significant as it determines the distance between BOPs used to quantify molecular motion from in TVD experiment. The components of g tensor are still subject to fitting, at least its rhombic component which is not negligible as it is in case of hyperfine tensor.

### 2.2.2. Empirical parameters in temperature and viscosity dependences

Once the magnetic tensor components were determined, it is possible to calculate EPR spectra. The spectra simulation procedure based on tensor averaging for accounting of fast



motion, and SLE for slow rotational diffusion is used for calculation of empirical parameters **a** and **b** in the equation (9). For this purpose, a set of EPR spectra is calculated axially symmetrical case (that is, no rhombic component in hyperfine tensor). The shift of separation between BOPs in theoretical EPR spectra measured with different values of correlation time  $\tau$  and order parameter  $S$ , if plotted in logarithmic scale versus  $\tau S$  according to the formula (9), allows to calculate the parameter  $b$  from the slope of linear approximation, and parameter  $a$  from its intersection with ordinate axis (Tkachev, 2010).

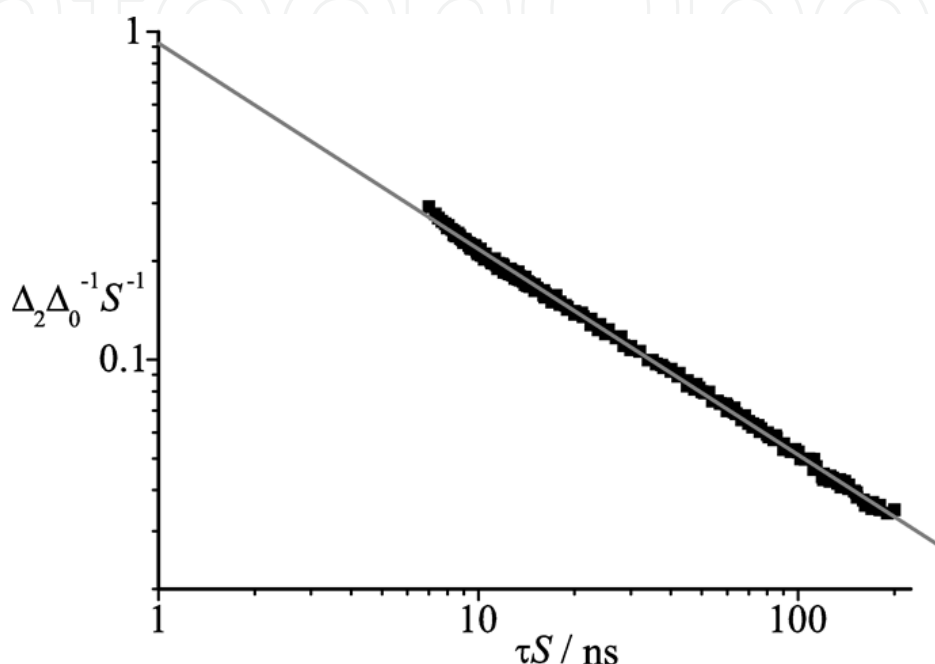


**Figure 2.** Theoretical dependence of BOP shift vs. global tumbling correlation time  $\tau$  and fast label motion order parameter  $S$ . It is used to find  $a$  and  $b$  parameters in equation (9). This particular dependence was calculated for  $g_{xx} = 2.0088$ ,  $g_{yy} = 2.0058$ ,  $g_{zz} = 2.0023$ ,  $A_{xx} = A_{yy} = 6.0$  G  $A_{zz} = 35.3$  G, and individual line width of 1.1 G. Every black point corresponds to simulated spectrum, and the gray line is least-square approximation.

Values of empirical TVD parameters determined from simulation of set of spectra according to the method described above are dependent on magnetic tensors and line widths used for calculation. High performance in spectra simulation which may be routinely achieved on modern workstations and personal computers makes possible to obtain these parameters interactively, upon changing line width or magnetic tensor components. This is important part of the EPR spectra interpretation method described here, as it may require multiple processing of experimental TVD data with different  $a$  and  $b$  values to achieve good coincidence of simulated spectra with experimental ones.

### 2.2.3. Experimental determination of $\tau$ and $S$ values

When empirical parameters are known, it is possible to use equation (11) for experimental data processing. According to equation (11), the dependence of  $2A'$  on  $(T/\eta)^{\frac{1}{b}}$  should be

linear. Therefore, an intersection of linear approximation of experimental results will give the value of  $2\bar{A}$  which encodes the order parameter according to expression (2). Then, from equation (9) it is possible to find the correlation time of slow global tumbling of the macromolecule.

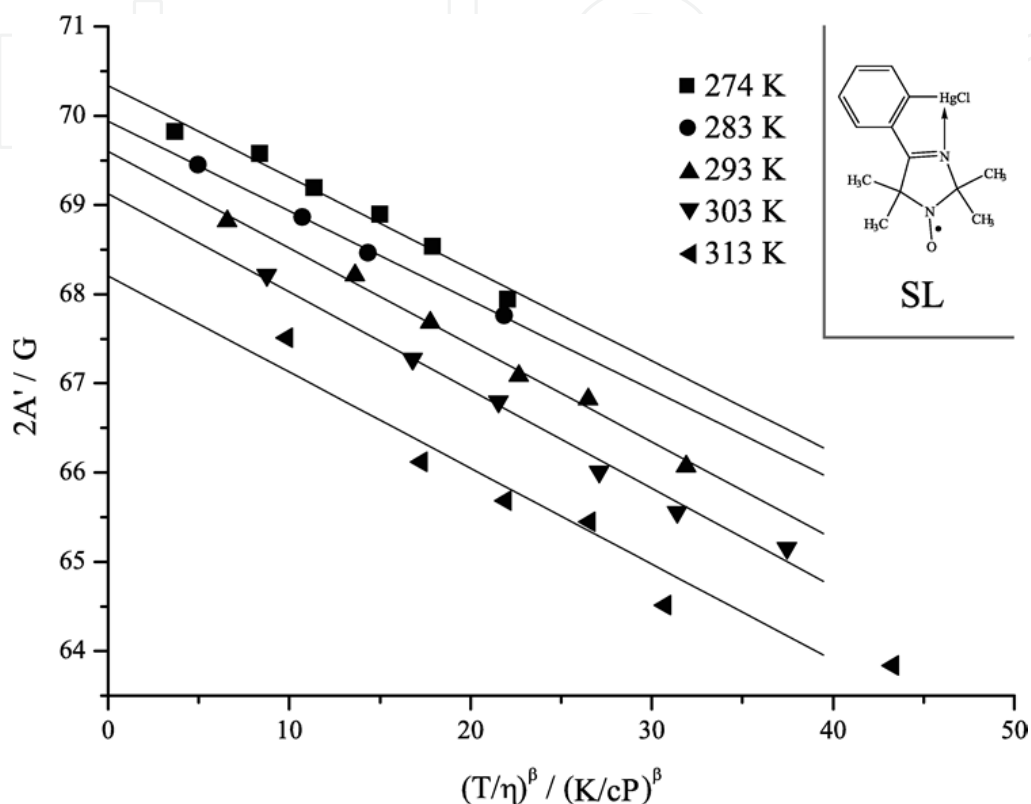


**Figure 3.** Typical plot of temperature and viscosity dependences of BOP separation. This data corresponds to bovine serum albumin (BSA) labeled with 4-(2-chloromercurophenyl)-2,2,5,5-tetramethyl-3-imidazoline- $\Delta^3$ -1-oxyl (on inset). It was used as model system for procedure test purposes. For every temperature the linear data approximation crosses ordinate axis on  $2\bar{A}$ , and order parameter value may be derived from it.

#### 2.2.4. Simulation of EPR spectra of spin-labeled macromolecules

The simulation of EPR spectra of spin-labeled macromolecules used here is also based on the two independent motions (TwIM) model (Dudich et al., 1977; Timofeev 1986; Timofeev & Samaryanov 1993, 1995; Tkachev 2009, 2010). Therefore, fast motion of the spin label relative to the macromolecule is taken into account by effective spin Hamiltonian partial averaging, and the slow motion of the macromolecule is determined by the rotational correlation time of isotropic diffusion.

By means of the generalized model of fast nitroxide oscillations the partially averaged magnetic tensor components can be calculated (Tkachev, 2009, 2010) in such a way that

order parameter obtained from TVD experiment can be employed. This is possible because axially symmetrical model presumed in TVD is a special case of the generalized model mentioned. Substitution of averaged tensors into the SLE-based procedure for slow motional nitroxide spectra simulations (Schneider & Freed, 1989) gives the final EPR lineshape with contributions of both fast and slow motions.

On the above basis the simulation program (S\_imult6) was developed. The model of fast limited oscillations (Timofeev and Samaryanov, 1995) gives formulas in analytical form by which components of partially averaged magnetic tensors can be calculated. According to model nitroxide fluctuates around some fixed axis  $\vec{n}$  defined in polar coordinates by  $\theta, \varphi$  angles. Fluctuations are limited by an angular amplitude of oscillation  $\alpha$ , and all orientations are equally probable in range from  $-\alpha$  to  $\alpha$ . However, it was shown (Tkachev 2009, 2010), that partially averaged magnetic tensors aren't diagonal in general case. This implies that tensors have to be diagonalized after averaging, resulting in tilt between principal axes of both partially averaged magnetic tensors to appear. Two parameters defining an axis of oscillation  $\vec{n}$ ,  $S = (3\cos^2\theta - 1)/2$ ,  $\kappa = (1 - 2\cos^2\varphi)$  can be shown to play role of order parameters. The meaning of  $S$  defined this way is exactly the same as in axially-symmetrical case which arises if one let  $\alpha = 180^\circ$ . In this case it is equal to experimental McConnell's order parameter. This allows using axially symmetrical case with experimentally determined order parameter as the starting point in scheme shown on Fig. 1, when calculating theoretical EPR spectra.

The general scheme for the resolution of the EPR spectroscopy inverse problem for spin-labeled macromolecules presented as follows. Experimentally determined magnetic tensor components, the correlation time  $\tau$  together with the order parameter  $S$ , found from temperature-viscosity dependences, are fed into the simulation procedure based on SLE (cycle 1 on Fig. 1). In axially symmetrical case one obtains a theoretical spectrum similar to experimental one only on its wings (position of BOPs). In order to fit calculated spectra to experiment in the central region of magnetic fields, it is necessary to deviate from initial  $\theta, \varphi$  and  $\alpha$  values, breaking axial symmetry (switch to cycle 2 on Fig.1). Additionally, the linewidth and initial tensor rhombic parts may be adjusted as well, to achieve the best fit of a theoretical spectrum to the experimental one. If these are modified, it may be necessary to recalculate empirical TVD parameters ( $a$  and  $b$ ), and repeat the procedure from cycle 1. Once it is possible to obtain consistent results from both cycles, process is complete. It utilizes the maximum of information from experimental TVD dependence, and yields the set of simulated spectra with the only difference in order parameters and macromolecular tumbling correlation time. The starting conditions are provided by axially symmetrical data obtained directly from experiment. This eliminates most of non-uniqueness which the usual multidimensional fitting procedures is prone to.

An ensemble may be inhomogeneous in sense of averaging parameters. One of the reasons for this is existence of macromolecule's structure fluctuations, or set of different structural conformations of the labelling site. This leads to concept of sub-ensembles of nitroxides,

called clusters (Timofeev & Samarianov, 1995). They are clustered according to averaging order parameters (all kinds of equivalent dynamical behaviors, producing identical averaged tensors), and these may be assumed to be normally distributed. The spectrum depends on  $\alpha(\alpha_0, \sigma)$ , where  $\alpha_0$  is an average, and  $\sigma$  is a standard deviation of the Gaussian distribution (Tkachev, 2010, Timofeev & Samarianov, 1995). The resulting spectrum is calculated as Gaussian-weighted sum of spectra of individual clusters. This adds single fitting parameter, but in many real-world cases helps to dramatically improve fits quality.

### 3. The temperature and viscosity dependences for spin-labeled Barstar in solution

Spin labeling, EPR and all the method described above, based on the temperature-viscosity dependence experiment, was used to study the protein-protein interaction between the enzyme barnase (Bn) and its inhibitor barstar (Bs) (Timofeev et al., 2008). A mutant of barstar (C40A), containing only one cysteine residue, C82 was selectively modified by spin label (SL) 4-(2-chloromercurophenyl)-2,2,5,5-tetramethyl-3-imidazoline- $\Delta^3$ -1-oxyl (Shapiro et al., 1979). We used spin label which ensured higher ability of his reporter group to access different protein microenvironments. To estimate the mobility of the spin labeled C82 side group and the whole globular protein quantitatively, the temperature-viscosity approach was used.

To extract unambiguous information from experimental EPR spectra of spin-labeled macromolecules, it is necessary to have maximum possible control over the degrees of freedom (DOFs) an EPR line shape depends on. This effectively reduces linehape 'degeneracy' with respect to the set of parameters used to interpret these spectra. Generally, for complex objects like mutually interacting proteins, unequivocal interpretation of EPR spectra is possible only when BOPs are present. For small molecules undergoing relatively rapid rotations narrowing the spectrum at ambient temperatures, decreasing the temperature and increasing solvent viscosity increase order parameters, as well as macromolecule tumbling correlation time. This leads to broad outer peaks (BOPs) of increasing amplitude to appear in low and high field regions of EPR spectra. By processing a series of EPR spectra of spin-labeled samples and measuring the separation between the BOPs, one can estimate the effective rotational correlation time  $\tau$  of the protein molecule and the order parameter  $S$  of the spin label attached to the side chain. EPR spectra of Bs-SL in solution with changing viscosity are shown on Fig. 1 and Fig. 2. Viscosity was controlled by addition of sucrose.

As can be seen from Fig. 4 and Fig. 5, BOPs shifts considerably towards field range end points with increasing viscosity, and this is an effect one expects to be able of studying temperature-viscosity dependence. According to formulas (11) for parameter  $2A'$ , this dependence is shown on Fig. 6.

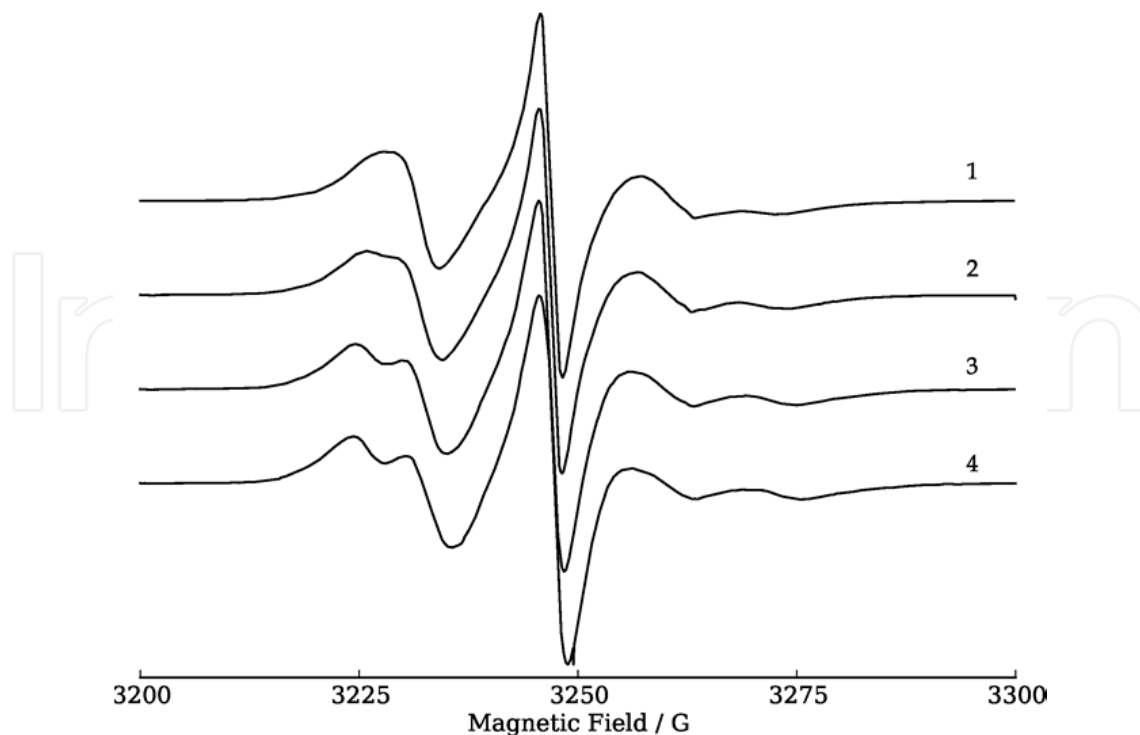


**Figure 4.** EPR spectra of Bs-SL at 1° C, with viscosity altered by addition of (1) 0%, (2) 6%, (3) 16%, and (4) 19.5 % sucrose (w/w).

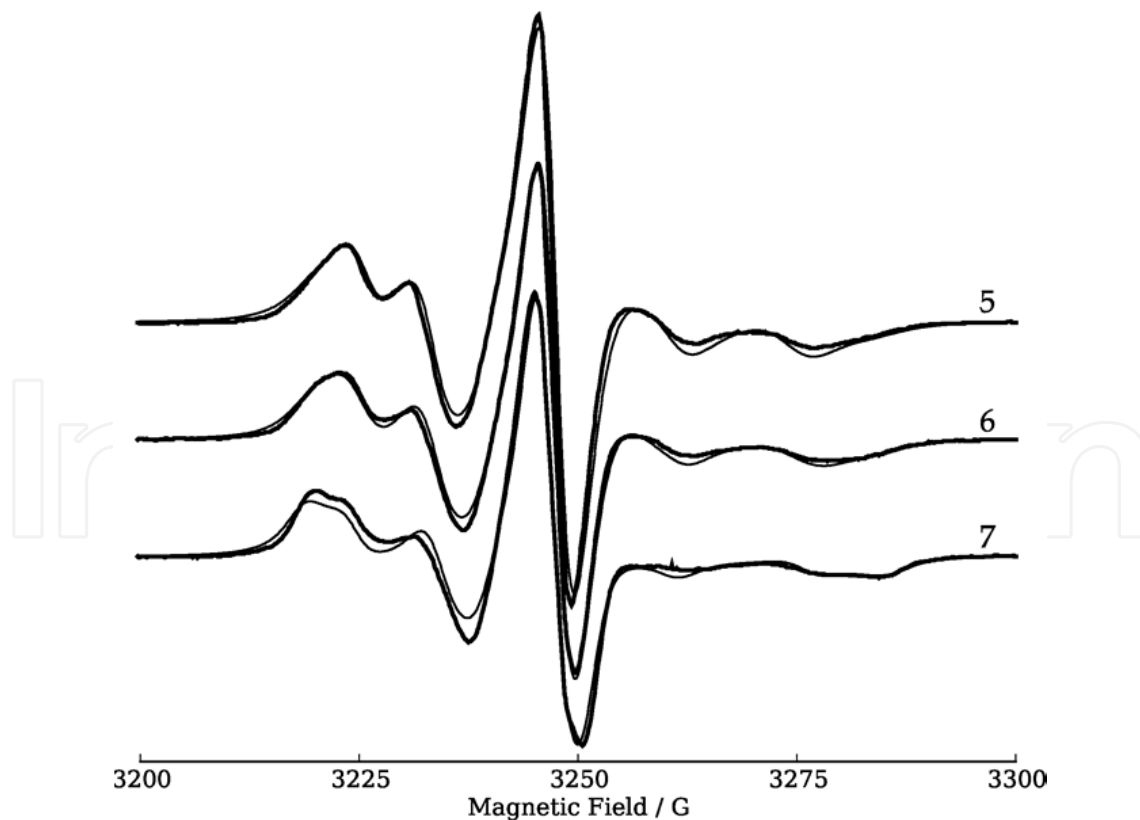


**Figure 5.** EPR spectra of Bs-SL at 1° C, with viscosity controlled by addition of (5) 27 %, (6) 33 %, (7) 40 % sucrose (w/w). The experimental spectrum is plotted with heavy line and the simulation - with fine line. The theoretical calculation of spectra shown is discussed in the text.

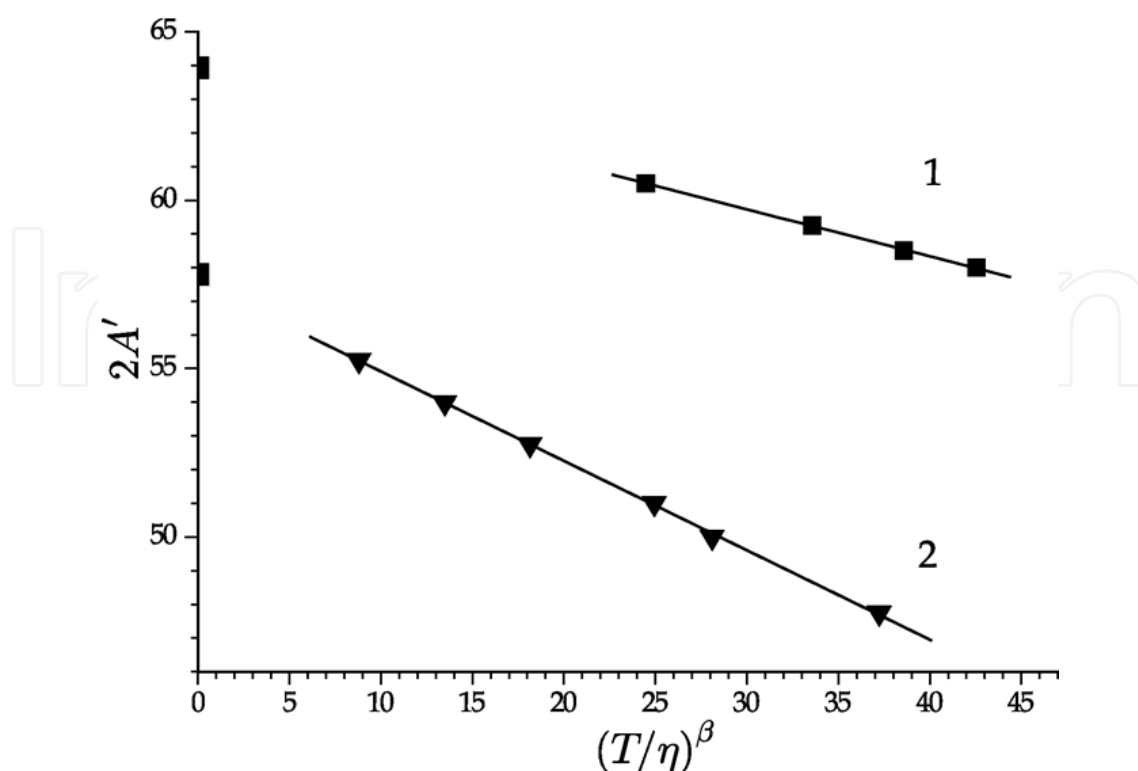


**Figure 6.** Temperature-viscosity dependences of separations between BOPs ( $2A'$ ) in the EPR spectra of Bs-SL (line 2), and complex Bs-SL with Bn (line 1) at 1° C. The data were fitted using the linear least squares method. Line 1 crosses the ordinate axis yielding the extrapolated value  $2\bar{A} = 63.9$  G, whereas line 2 yields  $2\bar{A} = 57.8$  G. Units are T for K, and cP (centipoises) for  $\eta$ . The value of TVD parameter  $\beta = 1/b = 0.74$ .

It is clearly observable from EPR spectra presented in Fig. 4 and Fig. 5, that at lower viscosity values (6%, 16%, and 19.5% w/w sucrose in solution) BOPs are considerably asymmetrical. In fact, there are two poorly resolved BOP pairs, what is clearly seen in spectra at higher viscosities (27%, 33%, and 40% w/w sucrose in solution). Therefore, it is clear that spectra are composed of two components, first broad, and second, narrower. The separations between BOPs from narrow component (three points)  $2A'$  are shown on the Fig. 6 (line 2). The first spectrum on Fig. 4 lacks of low-field BOP, thus there is no point for 0% sucrose on the line 2 (Fig. 6). At higher viscosity values (27%, 33%, and 40% sucrose in solution) BOPs from broad and narrow spectrum components were separated. Hence we define the separations between BOPs near to the center of the spectrum as  $2A'$  (narrow) and farther from the center of the spectrum as  $2A'$  (broad). As for the three points to  $2A'$  (broad) they are visible on the line 2 (Fig. 7). In Fig. 7 for clarity, a line 1 is repeated as line 1 in Fig. 6.

For these double-component spectra, two explanations are possible. This is either due to the Bs-Bs interaction of two macromolecules (Timofeev, et al., 2008), or a spin label SL have two dynamic states with strongly different order parameters. To clarify this alternative, an experiment on the binding of macromolecules Bs-SL with adsorbent has been undertaken.

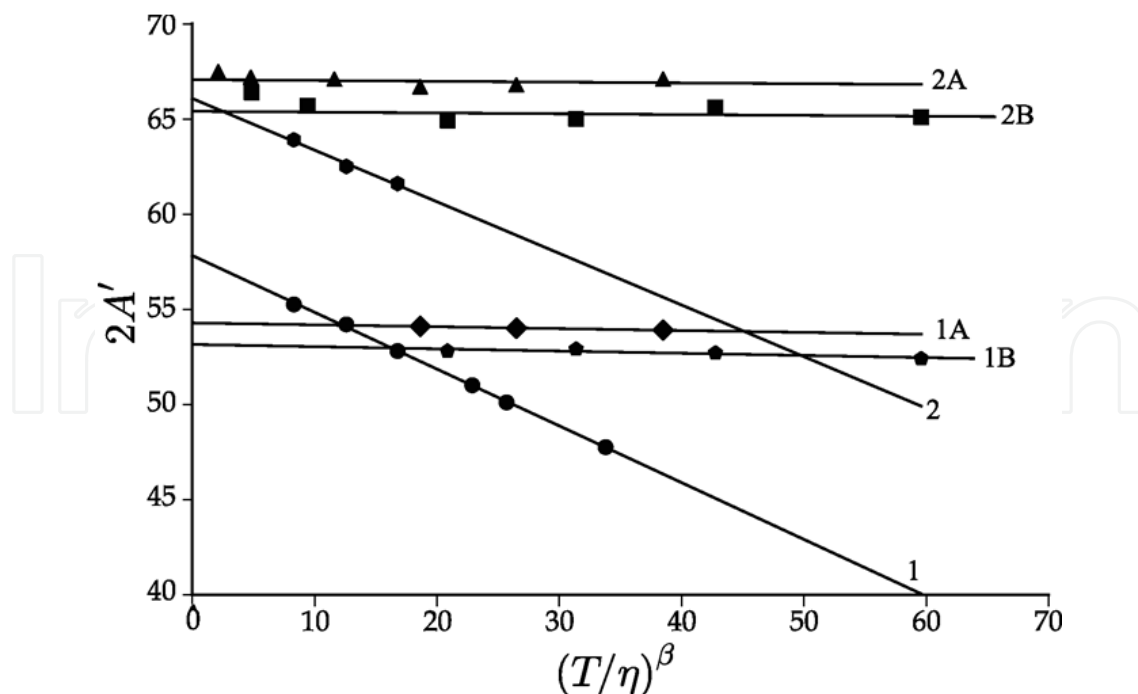


**Figure 7.** Temperature and viscosity dependences for BOPs separation ( $2A'$  /G) in EPR spectra of spin-labeled Barstar in solution, and on adsorbent. Solution: 6 points for BOPs from narrower component (line 1): (1) 6%, (2) 16%, (3) 19.5 %, (4) 27%, (5) 33%, and (6) 40 % sucrose (w/w), and 3 points for broad component BOPs (line 2): (1) 27%, (2) 33%, and (3) 40 % sucrose (w/w), at 1°C. With adsorbent: **1A** line at 1°C and **1B** line at 20°C for narrow component BOPs; **2A** line at 1°C and **2B** line at 20°C for broad component BOPs. The data were fitted using the linear least squares method. Line 1 crosses the ordinate axis yielding the extrapolated value  $2\bar{A} = 57.8$  G, and line 2 yields  $2\bar{A} = 66.1$  G. The value of  $\beta = 1/b = 0.74$ .

#### 4. The temperature and viscosity dependences for immobilized Barstar

If macromolecule with spin label attached to it can be immobilized, rendering effective correlation time to be large enough to mimic rigid-limit spectrum. In case with spin labeled Barstar we used QFF sepharose to achieve this goal. The sample was prepared by addition of SL to Barstar solution in HEPES buffer, then added 6 mg SL corresponding concentration to have molar excess of protein. Then 200 ml of QFF sepharose suspension was added and sample washed to remove unbound protein by spinning on microcentrifuge. Spin-labeled protein-charged sepharose was used for recording of EPR spectra. Temperature dependence of these spectra (1, 10, 20, 30, 40°C) without sucrose is shown on Fig. 8.

It is clear that all five EPR spectra display "quasi-powder" pattern (broad due to strong immobilization) as spin-labeled macromolecules are now attached to an adsorbent (cf. Fig.1). Over entire temperature range (1-40°C) two components are clearly observable, with corresponding BOP separations of  $2A'$  (narrow) and  $2A'$  (broad).

Rotational Brownian motion of medium-sized macromolecules in solution is on the nanosecond range. Linking macromolecules to an adsorbent shifts it to the microsecond range, which, in fact, is not distinguishable from rigid-limit ("powder spectrum") at

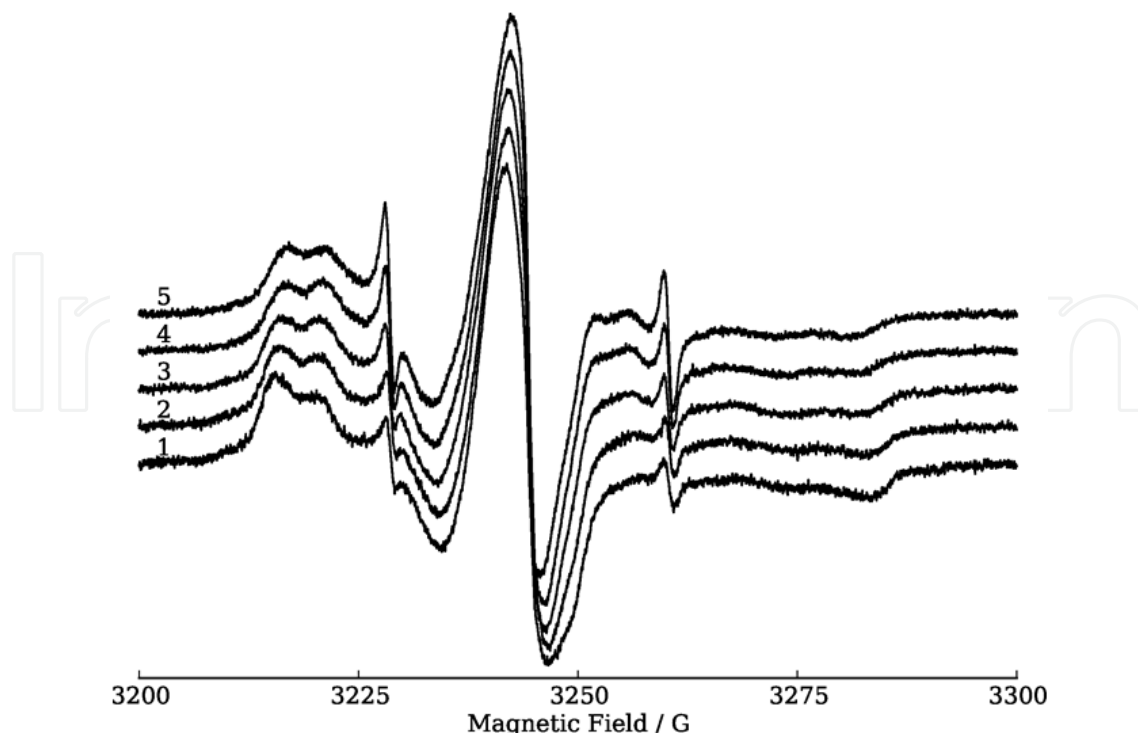


**Figure 8.** EPR spectra of the QFF-Bs-SL1 complex at 1°C (1), 10°C (2), 20°C (3), 30°C (4), and 40°C (5). The spectral width is 100 G.

experimental conditions used. Therefore, the shape of "quasi-powder" EPR spectrum is exclusively determined by the fast reorientation of the spin label in a limited configuration/conformation space. This makes it easy to measure the order parameter of nitroxide (see expression (2)).

On the other hand, once the protein is adsorbed on the sepharose, the arising "quasi-powder" EPR spectrum should not depend on oligomeric state of the protein, to an extent local structure of the protein close to labeling site is disturbed by weak inter-macromolecule interactions. Strong Barstar interaction with an heavily charged adsorbent is expected to significantly impair its ability to form dimer, and is expected to shift equilibrium to monomeric form. Therefore, we conclude that the order parameter  $S$  in the dimeric form of the protein (if any) and its monomeric form should be the same. Consequently, there are two conformational states of the spin label attached to the thiol group of the protein, corresponding to two spectral components with BOP separations of  $2A'$  (narrow), and  $2A'$  (broad).

In further experiments EPR spectra of Bs-SL on the adsorbent at different viscosities have been recorded, for the full temperature-viscosity dependence to be obtained. Corresponding spectra, for different temperatures, are shown on Figure 9 (A, B). Two components found (two BOP pairs) were processed independently to get order parameters for both spin label conformational states. Fig. 7 displays TVD for sepharose-bound Barstar overlaid on these for free protein in solution at 1°C (lines 1A and 2A) and 20°C (lines 1B and 2B). As seen in Fig. 7, four lines (1A, 1B, 2A, 2B) are parallel to the x-axis. This behavior is expected, as both types of BOPs (from narrow and broad spectrum components) do not shift with increasing viscosity of the medium in the "quasi-powder" EPR spectra, given the value of  $\tau$  for protein



is virtually infinite. Consequently, the separations between BOPs not change and, thus, in the case with adsorbent:  $2A'$  (narrow) =  $2\bar{A}$  (narrow) and  $2A'$  (broad) =  $2\bar{A}$  (broad). It also means that the second term in equation (1), for both spectrum components is zero.

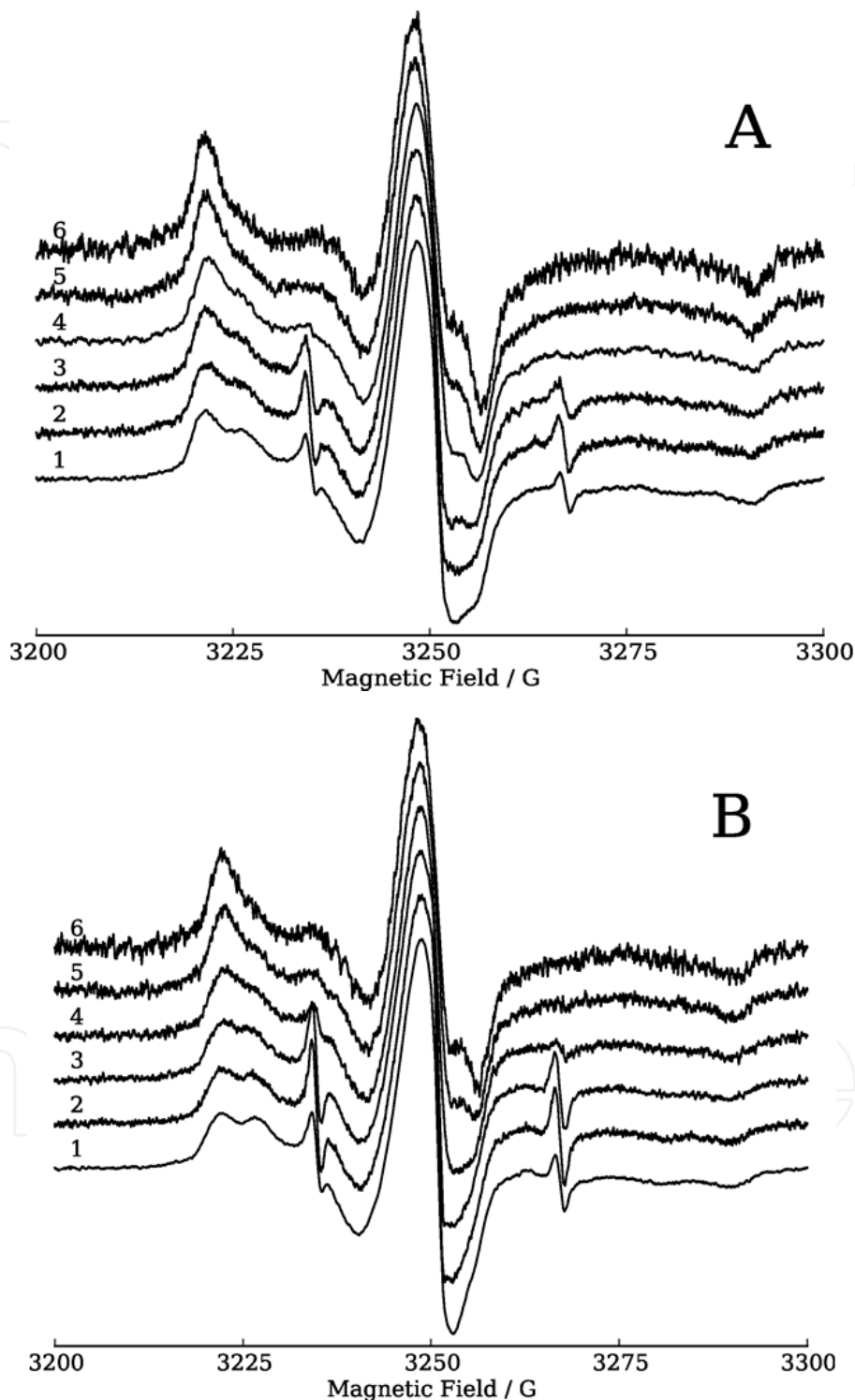


**Figure 9.** EPR spectra of spin labeled Barstar immobilized on QFF sepharose (QFF•Bs-SL system) at 1°C (A) and 20°C (B) with viscosity altered by addition of (1) 0%, (2) 15%, (3) 30%, (4) 37%, (5) 48%, and (6) 56% sucrose (w/w).

It is now straightforward, knowing  $2A_{ZZ}$  and  $2a_0$ , to calculate order parameters  $S_1$  (for narrow component) and  $S_2$  (for broad component) according to the formula (2) for both states of the spin label. Dependences of the order parameters  $S_1$  and  $S_2$  on the temperature are shown in Fig. 7, in this case  $S_2 > S_1$ .

Thus the ensemble of spin-labeled molecules barstar Bs-SL is divided into two sub-ensembles. In one sub-ensemble spin label is found in 1<sup>st</sup> state with corresponding order parameter  $S_1$ , and another – in 2<sup>nd</sup> state with order parameter  $S_2$ .

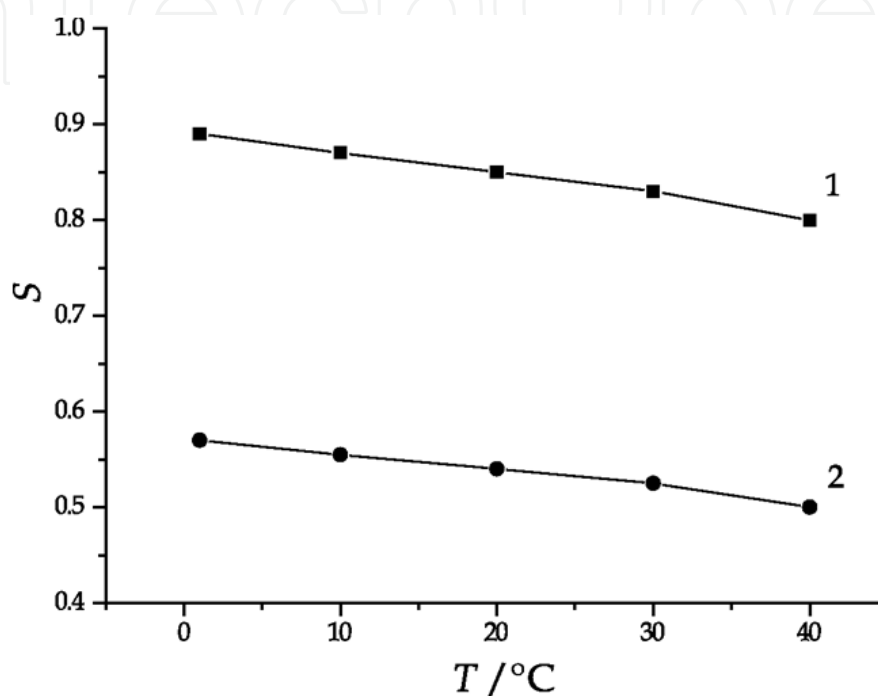


**Figure 10.** Values of the order parameters  $S_2$  (to 2<sup>nd</sup> state of SL, farther BOPs) – line 1; and  $S_1$  (to 1<sup>st</sup> state of SL, near BOPs) – line 2; in depend on the ambient temperatures.

Interestingly, the fast motion activation by temperature in each of the SL states in a local protein site (Cys82) is negligible. As seen in Fig. 7, parameters  $S_1$  or  $S_2$  drift only slightly over entire temperature range from 1 to 40°C. This suggests that the rigid spin label samples almost the same amount of configuration space provided by rigid protein frame in this range of temperatures.

Addition of the Barnase (Bn) to Bs-SL solution results in a temperature-viscosity dependence, as shown in Fig. 3 by line 1. In this case, the spin label in the complex of BnBs-SL has a single state with a value of the order parameter ( $S = 0.86$ ). Line 1 slope is two times less than that of line 2 (Fig. 3). Very strong affinity of Barstar to Barnase explains this, since the molecular weight of BnBs complex (22.7 kD) is about twice larger than the molecular weight of Barstar (10.3 kD).

When introduced to the system QFF•Bs-SL, Barnase had no significant effect on EPR spectrum (see Fig. 8). In case of stable Bn•Bs-SL complex formation, the EPR spectrum was expected to be substantially changed, which is the case in solution. The capacity of the QFF sepharose which is abundant in the sample mixture and its charge make Bn easier to bind to

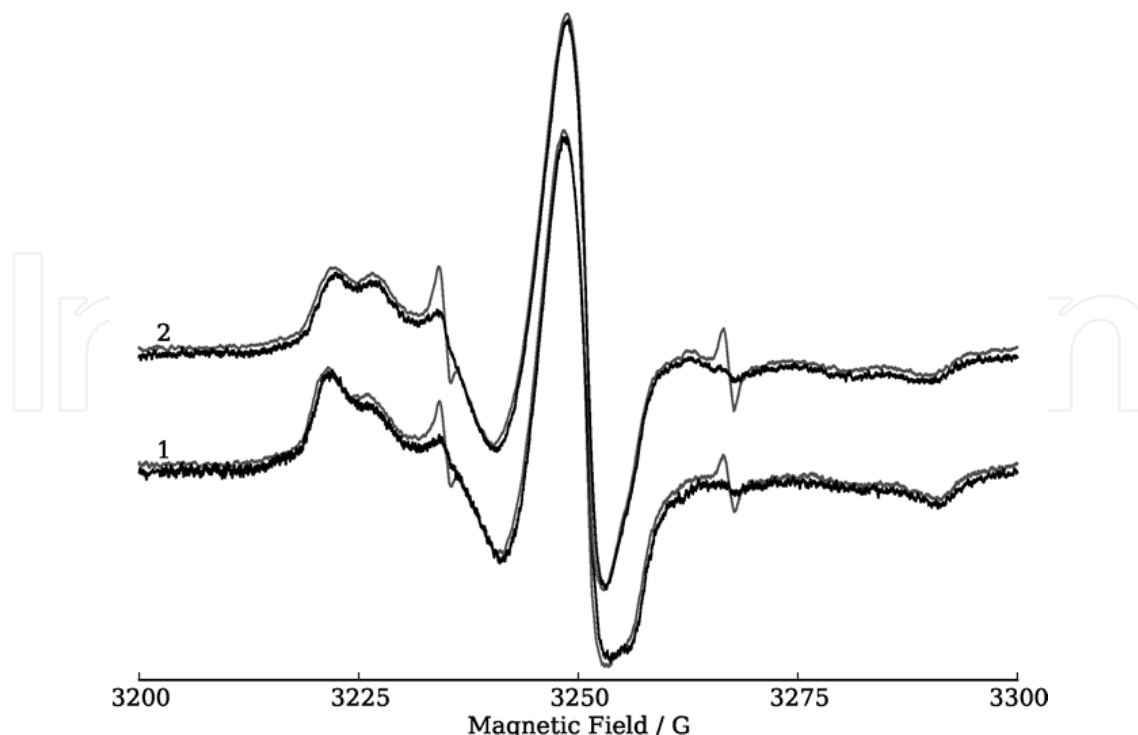


**Figure 11.** The spectra EPR of QFF-Bs-SL (light line with sharp peaks of free SL) and the same at adding Bn in a bit large excess (dark line without sharp peaks) at 1°C (1) and 20°C (2).

the adsorbent, while bound Barstar may have its Bn binding interface unreachable. This leads to disruption of Bn•Bs-SL complex formation equilibrium. No change in EPR spectra at two temperatures, 1°C and 20°C indicate that there is apparently no significant amount of complex present. Smaller amount of free label (three narrow lines on Fig. 8) after Bn addition was due to centrifugation, and, therefore, better washing.

## 5. Spin-labeled Barstar EPR spectra simulation

The procedure for simulating EPR spectra using the proposed model of the two motional nitroxide radical was described in section 2.3. Here we want to give some examples of EPR spectra simulation, paying an attention to the similarity of theoretical spectra to experimental ones.

### 5.1. Barstar and formation of complex with Barnase

On the Fig. 5 (A, B, C) fitted simulation EPR spectra superimposed onto experimental ones. As it appears, they can be described by two dynamical states of spin label rapid motion relative to Barstar molecule. If one assumed these states uncoupled, each of them corresponds to its own EPR spectrum, and experimental one corresponds to their weighted sum. On Figures 12 - 14 individual simulated spectra are shown for each state of spin label (1<sup>st</sup> and 2<sup>nd</sup>); their superposition results a final spectrum. Using Gaussian distribution on  $\alpha$  averaging parameter helps to obtain better fit due to states dynamical coupling (exchange), and the spectra shown on these figures actually account for it this way (see legends).

We used following initial components of nitroxide magnetic tensors:  $g(X,Y,Z) = 2.00732; 2.0063; 2.0022$ ;  $A(X,Y,Z) = 6.55 \text{ G}; 5.00 \text{ G}; 35.40 \text{ G}$ . In legends to figures, the rotational correlation times and linewidth, parameters used for calculation of partially averaged tensors components along with themselves, are given.

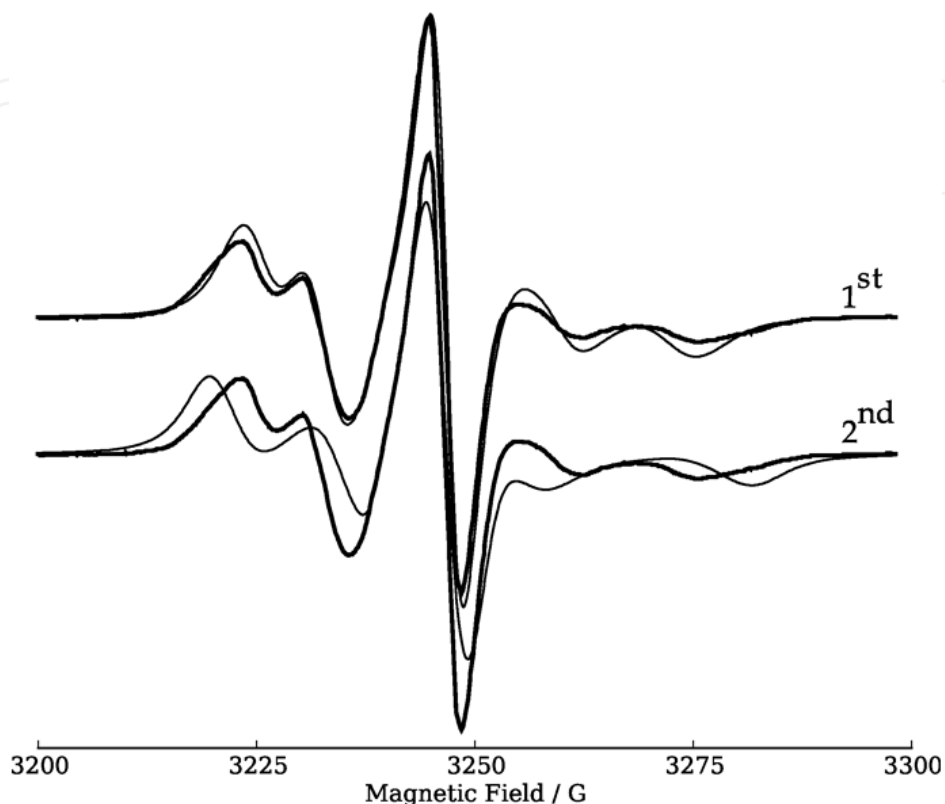


**Figure 12.** Simulated EPR spectra (fine line) for of 1<sup>st</sup> state SL and 2<sup>nd</sup> state of SL in comparison with an experimental spectrum of Bs-SL at 1° C and 27 % sucrose in solution (heavy line).

Spectrum for of 1<sup>st</sup> state contains BOPs close to the center (narrow). It is described by three parameters which, according to section 2.3, determine partial averaging of tensors in 1<sup>st</sup> state by the values of  $\alpha = 77(15)^\circ$ ,  $\theta = 46^\circ$ ,  $\phi = 5^\circ$ . Each spectrum was calculated as the average by  $\alpha$  with Gaussian distribution, as 77(15), where the value in brackets is the standard deviation. Magnetic tensors diagonal components:  $\bar{g}(X,Y,Z) = 2.00696, 2.00562, 2.00323$ ;  $\bar{A}(X,Y,Z) = 6.66246 \text{ G}, 11.9003 \text{ G}, 28.3872 \text{ G}$ . BOPs in simulated EPR spectrum (fine line) for 2<sup>nd</sup> state located farther from the center. This second state is described by parameters  $\alpha = 30(44)^\circ$ ,  $\theta = 30^\circ$ ,  $\phi = 5^\circ$ . Magnetic tensors diagonal components:  $\bar{g}(X,Y,Z) = 2.00723, 2.00628, 2.0029$ ;  $\bar{A}(X,Y,Z) = 6.46487 \text{ G}, 5.74586 \text{ G}, 34.7363 \text{ G}$ . Rotational correlation time for macromolecule was  $\tau = 25 \text{ ns}$ . Linewidth used was 1.7 G. The simulated spectra in both states were summed with the ratio of 28:72, which gives the resulting spectrum shown in Fig. 5(5).

All partial averaging parameters are the same as in the legend to Fig. 12. The protein rotational correlation time is  $\tau = 38 \text{ ns}$ . The simulated spectra in both states were summed with the ratio of 45:55, which gives the resulting spectrum shown in Fig. 5(6).

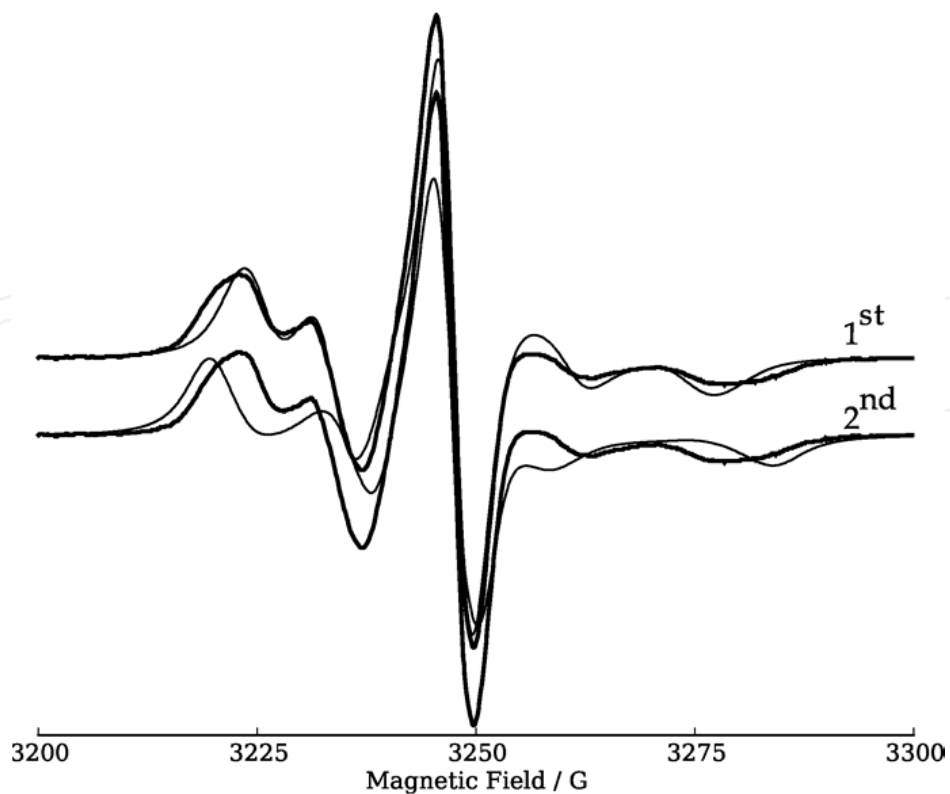


**Figure 13.** Simulated EPR spectra (fine line) for 1<sup>st</sup> and 2<sup>nd</sup> states of SL and 2 state SL in comparison to experimental one of Bs-SL at 1° C and 33 % sucrose in solution (heavy line).

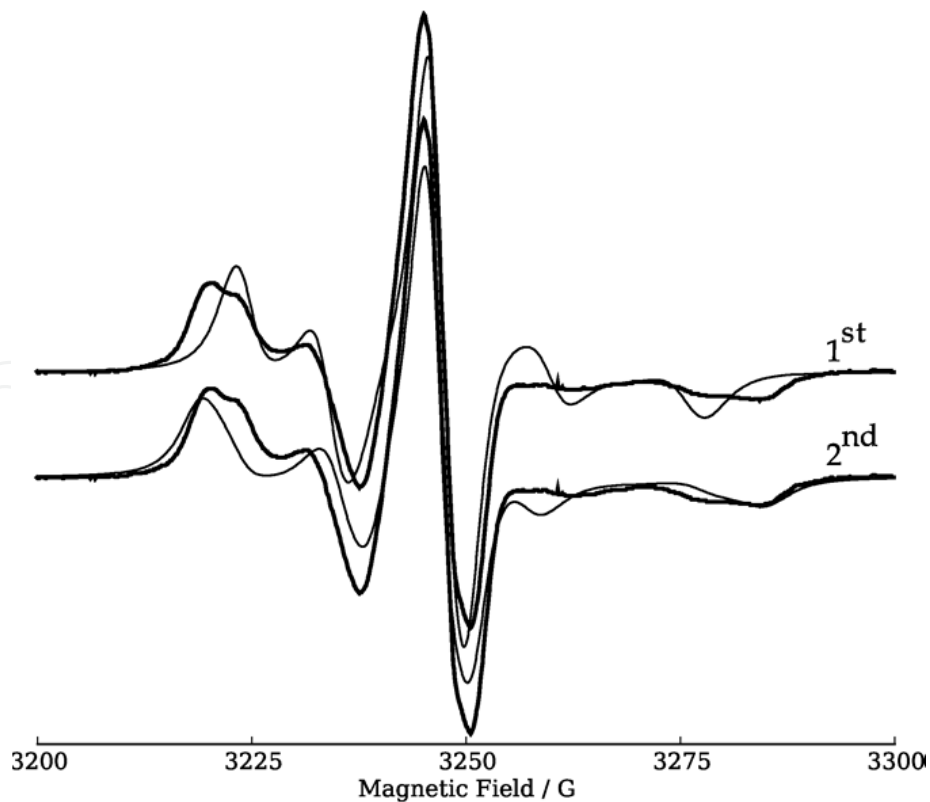


**Figure 14.** Simulated EPR spectra (fine line) for 1<sup>st</sup> and 2<sup>nd</sup> states of SL and 2 state SL in comparison to experimental one of Bs-SL at 1° C and 40 % sucrose in solution (heavy line).

All partial averaging parameters are the same as in the legend to Fig. 12. The protein rotational correlation time is  $\tau = 60$  ns. The simulated spectra in both states were summed with the ratio of 40:60, which gives the resulting spectrum shown on Fig. 5 (7).

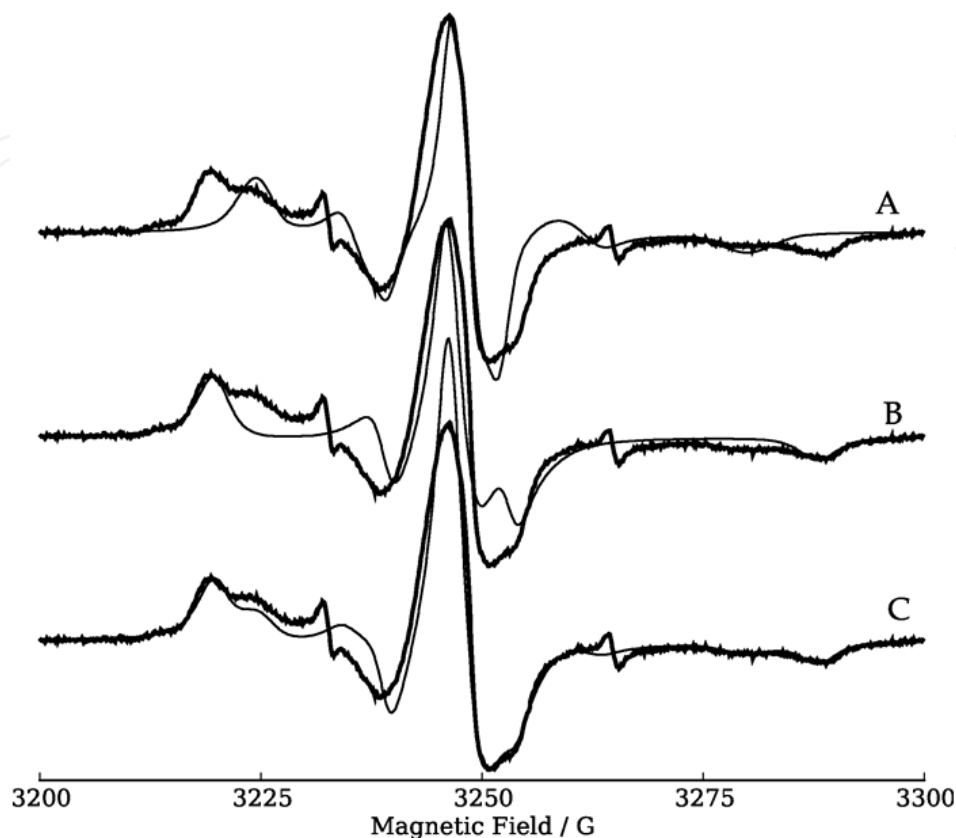


**Figure 15.** EPR spectrum of QFF-sepharose-Bs-SL at 1° C and 0 % sucrose (heavy line) and the simulated spectrum of 1<sup>st</sup> or 2<sup>nd</sup> states (thin line). (A) The 1<sup>st</sup> state is described (see Fig. 9A) is described by three parameters which, according to section 2.3, determine partial averaging of tensors in 1<sup>st</sup> state by the values of  $\alpha = 77(14)^\circ$ ,  $\theta = 46^\circ$ ,  $\phi = 5^\circ$ . Components of averaged tensors:  $\bar{g}(X,Y,Z) = 2.00696, 2.00562, 2.00323$ ;  $\bar{A}(X,Y,Z) = 6.66246$  G, 11.9003 G, 28.3872 G. Each spectrum was calculated as the average by  $\alpha$  with Gaussian distribution, as 77(15), where the value in brackets is the standard deviation. The rotational diffusion tensor components (expressed as correlation times) for macromolecule are  $\tau_x = 100$  ns,  $\tau_y = 1000$  ns,  $\tau_z = 1000$  ns. Anisotropic linewidth components are  $\delta_x = 1.3$  G,  $\delta_y = 1.5$  G,  $\delta_z = 1.5$  G. (B) The 2<sup>nd</sup> state is described (see Fig. 9) by three parameter values of  $\alpha = 27(32)^\circ$ ,  $\theta = 27^\circ$ ,  $\phi = 5^\circ$ . Components of averaged tensors:  $\bar{g}(X,Y,Z) = 2.00724, 2.00629, 2.00226$ ;  $\bar{A}(X,Y,Z) = 6.66246$  G, 11.9003 G, 28.3872 G. The rotational diffusion tensor components (expressed as correlation times) for macromolecule are  $\tau_x = 100$  ns,  $\tau_y = 1000$  ns,  $\tau_z = 1000$  ns. Anisotropic linewidth components are  $\delta_x = 1.4$  G,  $\delta_y = 1.9$  G,  $\delta_z = 1.9$  G. (C) Spectrum of QFF-sepharose-Bs-SL at 1° C and 0 % sucrose in solution, (heavy line) and the simulated spectrum (fine line) obtained by summation of ones for 1<sup>st</sup> and 2<sup>nd</sup> states (Fig. 15 A, B), with ratio of 30:70.

The results obtained by fitting of simulated spectra to experimental ones for spin-labeled Bs-SL, are listed in legends to Figures 12, 13, 14. Thus, three points (27, 33 and 40% sucrose) on temperature-viscosity dependence (Fig. 6 line2; or Fig. 7 line1) correspond to simulated EPR spectra on Fig. 5 and Fig. 12, 13, 14. It is important to note that simulated EPR spectra differ

solely in the rotational correlation time of macromolecule! This is highly consistent with proposed TVD advantage of separating BOPs shift contributions regarding to slow rotational dynamics of macromolecule, and rapid motion of spin label. The partial averaging of magnetic tensors conserve when temperature is held at constant level.

## 5.2. Sepharose-immobilized spin-labeled Barstar EPR spectra

The EPR spectra of Bs-SL in solution in the presence of QFF sepharose on Fig. 8 and Fig. 9 are shown. This entire set of spectra can be simulated using the same principle described here. However, for an example we have selected only two experimental spectra to show procedure of simulation (see section 2.2.4). We will discuss already shown simulated EPR spectra of Bs-SL in solution.

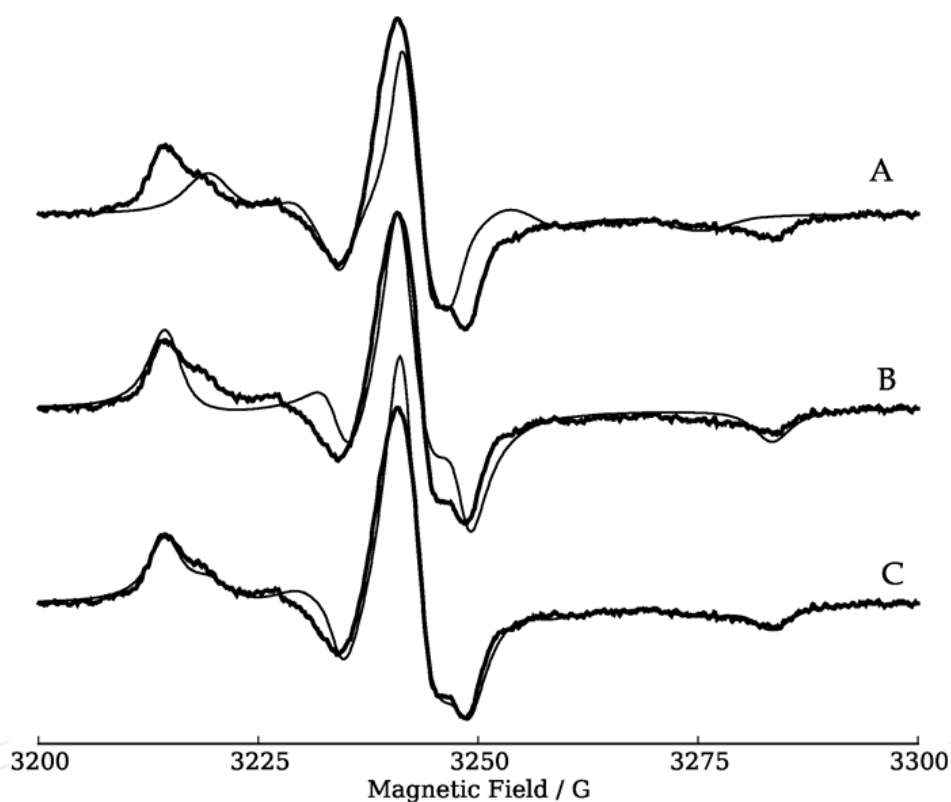


**Figure 16.** A. EPR spectrum of QFF-sepharose-Bs-SL at 1° C and 35% sucrose in solution (heavy line), and the simulated spectrum of 1<sup>st</sup> (fine line). Partial averaging parameters are the same as given in legend to Fig. 15A. The rotational diffusion tensor components (expressed as correlation times) for macromolecule are  $\tau_x = 200$  ns,  $\tau_y = 1000$  ns,  $\tau_z = 1000$  ns. Anisotropic linewidth components are  $\delta_x = 1.5$  G,  $\delta_y = 2.4$  G,  $\delta_z = 2.4$  G.

B. Spectrum of QFF-sepharose-Bs-SL at 1° C and 35% sucrose in solution (heavy line) and the simulated spectrum of 2<sup>nd</sup> state (fine line). Partial averaging parameters are the same as given in legend to Fig. 15A. The rotational diffusion tensor components (expressed as correlation times) for macromolecule are  $\tau_x = 200$  ns,  $\tau_y = 1000$  ns,  $\tau_z = 1000$  ns. Anisotropic linewidth components are  $\delta_x = 2.0$  G,  $\delta_y = 3.0$  G,  $\delta_z = 2.0$  G.

C. EPR spectrum of QFF-sepharose-Bs-SL at 1° C and 35 % sucrose in solution, (heavy line) and the simulated spectrum calculated as weighted sum of the above with ratio of 30:70.

On the Fig. 16, experimental spectra of QFF-sepharose-Bs-SL at 1° C and 35 % sucrose in solution, (heavy line), are shown along with simulated ones, demonstrating individual contributions from two SL states. The final spectrum (weighted sum of two states) is shown on Fig.15

### 5.3. Fast motion analysis by Molecular Dynamics

Method of Molecular Dynamics (MD) has become a very powerful and versatile tool for research connected with protein dynamics. Significant growth of hardware computational capabilities recently makes it possible to incorporate MD simulations into many analysis workflows involving experimental data collected using modern physical methods. It is successfully used in conjunction with nuclear magnetic resonance (NMR) for elucidation of protein structure and dynamics. The spin labelling and EPR may provide similar type of information, in form of order parameters (although on different time scale). Conventional MD method itself is completely theoretical (that is, pure calculation with no use of experimental data regarding particular system), but it is attractive as it provides detailed information on the system (macromolecule) dynamics. As a result of MD run, one obtains a trajectory with the time course of all atomic coordinates of the system. Modern software and visualization hardware allows viewing the resulted trajectory, and one can see a visual representation of the molecular system in time, which makes this technique a powerful tool for analyzing the dynamic properties of macromolecules. The trajectory obtained from MD enables one to calculate virtually any property of the system. We suggest it is very attractive to join the MD method with EPR techniques, once the latter provide experimental data to be guidance for designing MD runs, and/or verifying its results. On the other side, MD calculations may help in interpretation of EPR spectra.

MD method was used here to study the internal structural and dynamical properties of spin-labeled Barstar and its complex with Barnase. It was already mentioned in section 2, that EPR spectrum gives 'digest' type of information about the system dynamics. Most efforts to bridge MD and EPR techniques are now focused on attempt to simulate EPR spectrum from MD trajectory. We adopt different approach, similar to one used in NMR, based on order parameters. As a quantitative estimate for comparing the results of the two methods we used parameter  $S$ , which characterizes the angular reorientations of the attached spin label and the spatial constraints of the immediate protein environment. This order parameter, easily and unambiguously determined from the temperature and viscosity dependencies, can be calculated from the MD trajectory. The order parameter was calculated in two ways from the MD trajectories: the McConnell's method (axially symmetrical case), and the method of Model Free approach.

The initial structure of barstar molecules with a resolution of 2.8 Å (PDB id 1A19) was obtained from the database Protein Data Bank. The structure was prepared for MD, Cys82 residue was mutated to spin-labeled cysteine. New residue SLHG was added to parameter



files used for simulation; the parameters were combined from (Stendardo E *et al.*, 2010), CHARMM-cgenff and UFF, and optimized to reproduce average geometry of spin label known from X-Ray (Shapiro A. B. *et al.*, 1979)). Explicit solvent model was used, with TIP3 water. After equilibration (NPT ensemble with Langevin method for temperature control), a series of annealing steps has been performed. Annealing ended up in clearly observable two kinds of distinct dynamical behavior of spin label, more and less ordered. For them, the production runs of lengths of 20 ns at 330 K, and 10 ns at 300 K, were performed.

The initial structure of the complex barnase-barstar (PDB id 1AY7) was also obtained from the Protein Data Bank. Spin-labeled complex was reconstructed by Targeted MD using already built model of labeled Barstar. Both dynamical states of spin label attached to Barstar, discovered by annealing, upon virtual Barnase 'binding', yielded trajectory with disordered motional state absent. Trajectories of length of 20 ns at 330 K and 10 ns at 300 K were calculated, and used for determination of order parameters.

All calculations were performed using the software packages NAMD & VMD (Phillips J.C., *et al.*, 2005; Humphrey W., *et al.*, 1996).

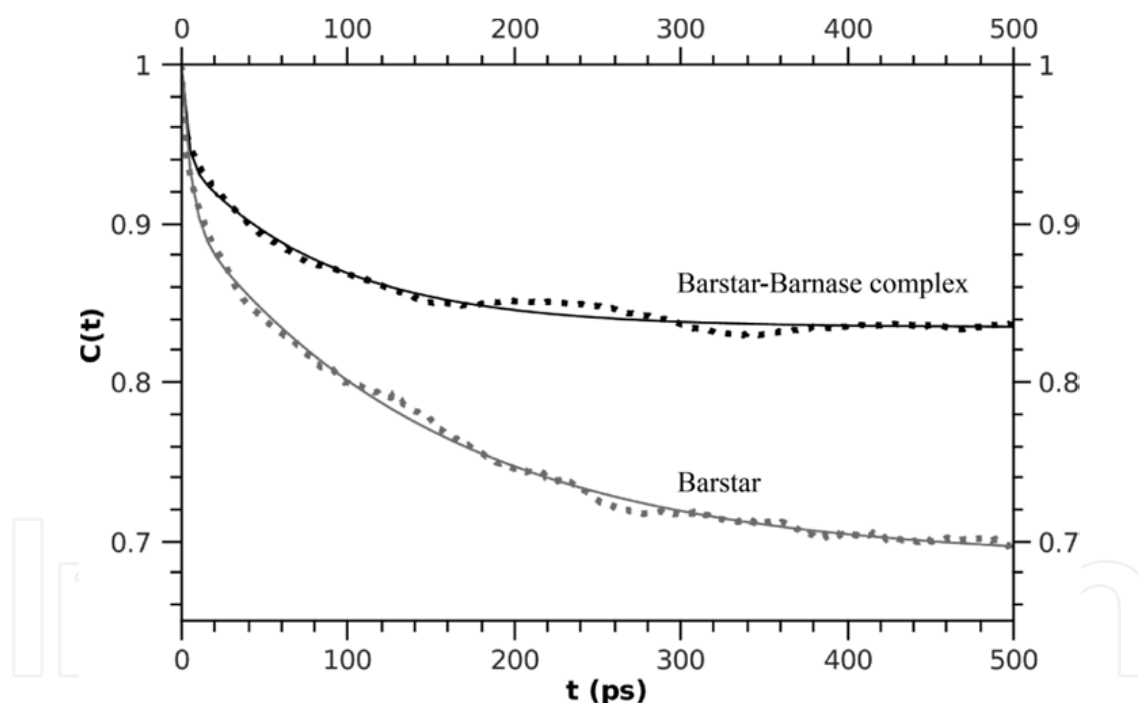


**Figure 17.** Autocorrelation function calculated from MD trajectories (squares) of Barstar (gray) and its complex with Barnase (black), and corresponding two-exponential model fits (line).

It is straightforward to compute coordinate autocorrelation function from MD trajectory. Its long time asymptotic limit is referred as generalized order parameter, as it does not rely on azimuthal motion symmetry, which is the case of McConnell's parameter  $S$ . This method of order parameter definition is commonly used in NMR and referred to as Model Free approach (Lipari, G.; Szabo, 1982; K.K. Frederick, K. A. Sharp., 2008). Two-exponential decomposition of autocorrelation function obtained for free Barstar yielded fast-component

order parameter (apparent correlation time 3.2 ns for Bs, or 5.4 for complex) to be significantly different from one for Barstar-Barnase complex (0.89 *vs* 0.97). McConnell's azimuthal order parameters calculated along entire trajectories were lower,  $S = 0.67$  for the Bs, and  $S = 0.93$  for the BnBs complex, which is consistent with motion anisotropy (azimuthal and generalized order parameters coincide when motion is axially symmetrical). The exact calculation by averaging along the trajectory shown  $S = 0.67$  for the free Barstar, and  $S = 0.93$  for the complex. This is expected, as all the EPR spectra for Barstar and its complex with Barnase presented above were simulated using non-axial model (but with several order parameters). On the other hand, the value of azimuthal order parameter  $S$  is in good agreement, as expected, with the experimental value obtained from the temperature-viscosity dependence of EPR spectra. The detailed trajectory analysis for free Barstar showed that it is non-uniform in sense of spin label motion. Namely, some parts of trajectory demonstrated much less disorder in this motion, and order parameter computed from them appeared to be 0.91, which is in good agreement with McConnell's order parameter determined experimentally by TVD for 2<sup>nd</sup> state EPR spectra component.

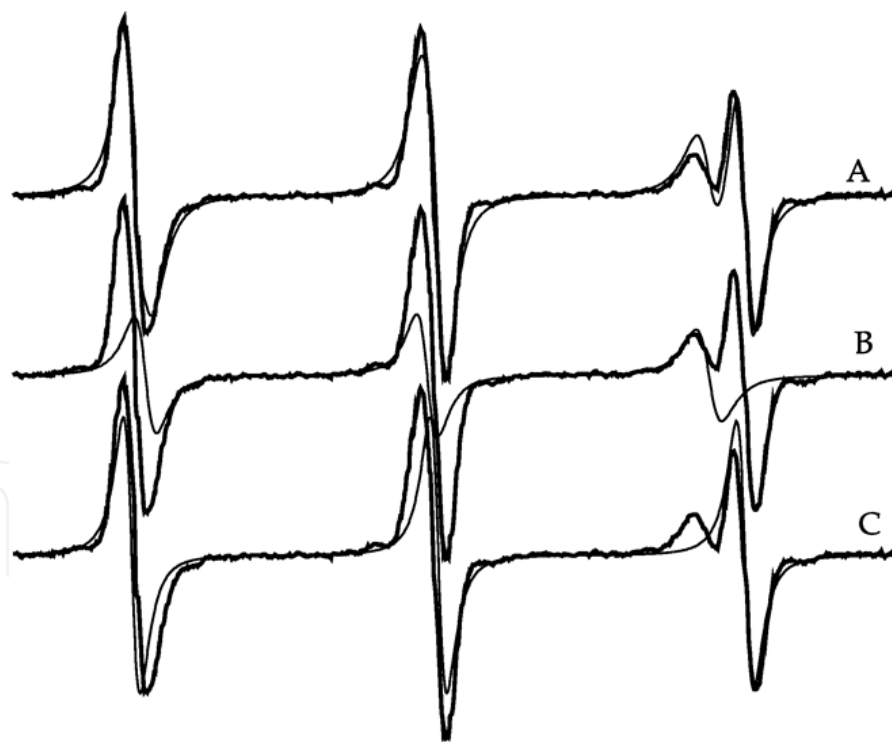


**Figure 18.** A. Experimental EPR spectrum of TEMPO radical in DPPC at 37.6°C (heavy line) and simulated spectrum (fine line) at X band (microwave frequency 9.15 GHz). All necessary parameters for simulation are summarized in Table 1. Center field  $B_0 = 3260$  G, and scan range is 49 G. B. The simulated EPR spectrum (fine line) of TEMPO radical in lipid phase. Parameters are in Table 1. C. The simulated EPR spectrum (fine line) of TEMPO radical in aqueous phase. Parameters are in Table 1.

## 6. Two motion model for EPR spectra simulation of TEMPO radical in membranes

The given approach can naturally be extended to membrane structures. On the Fig. 18, 19 calculated EPR spectra of TEMPO radical in DPPC in X- and W-bands, correspondingly, are shown. The experimental spectrum is taken from the excellent Smirnov's work (Smirnov et al., 1995). The experimental part of this work is highly valuable, but the interpretation of EPR spectra, from our point of view, should be conducted differently. We propose model, according to which, TEMPO radical, being in lipid phase, subjects to fast anisotropic reorientation, simultaneously experiencing the slow dynamic process motion due to lateral heterogeneity of domain structure in lipid bilayer.

Figures 18 and 19 represent the first example when simulated EPR spectra precisely reproduce experimental EPR spectra both in X and W bands, with exactly the same magnetic and dynamic parameters. The only simulation parameter changed was the frequency of EPR device. This consistency of our approach with multifrequency EPR data strongly argues for approach described here for uniform interpretation of dynamical effects in EPR spectra of spin-labeled samples.

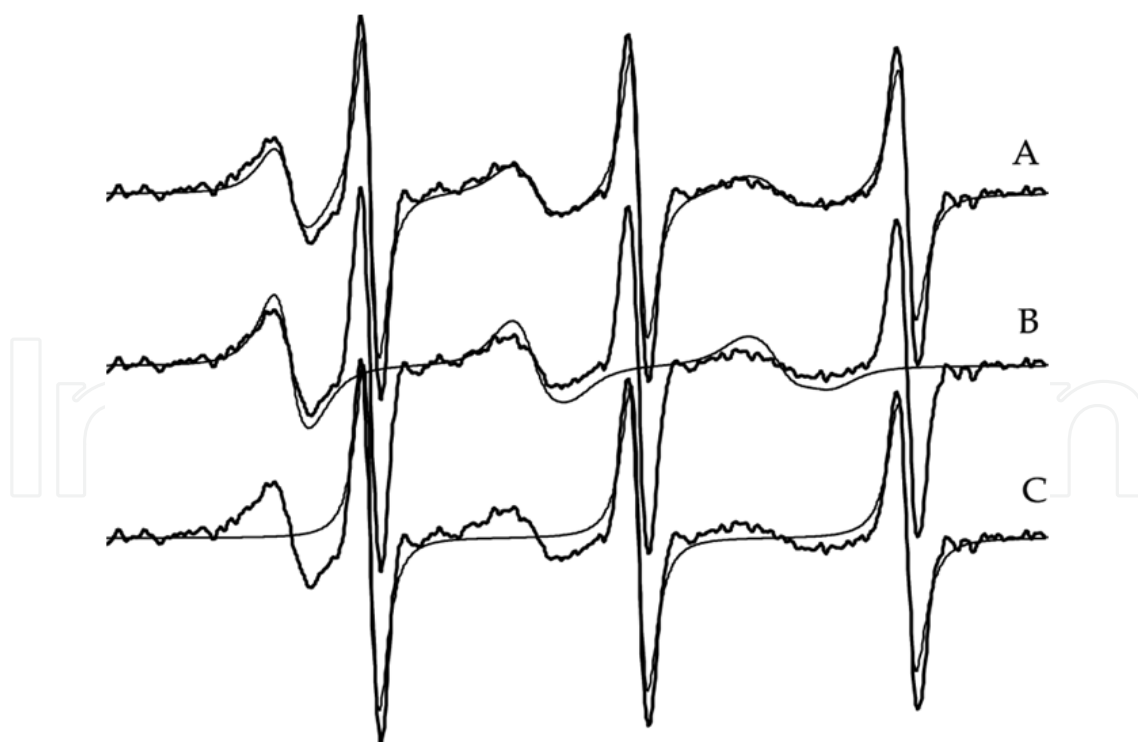


**Figure 19.** A. Experimental EPR spectrum of TEMPO radical in DPPC at 37.6°C (heavy line) and simulated spectrum (fine line) at W-band (microwave frequency 94.3 GHz),  $B_0 = 33584$  G, scan range is 60 G. B. The simulated EPR spectrum of TEMPO radical in lipid phase. Parameters are in Table 1. C. The simulated EPR spectrum of TEMPO radical in aqueous phase. Parameters are in Table 1.

Parameters	Water phase	Lipid phase
$g_x$	2.0093	2.0098
$g_y$	2.0063	2.0068
$g_z$	2.0022	2.00245
$A_x$	8.0 G	6.5 G
$A_y$	6.0 G	5.0 G
$A_z$	37.3 G	35.6 G
$\alpha$	1	173°
$\theta$	0	53°
$\phi$	0	45°
$\bar{g}_X$		2.006477
$\bar{g}_Y$		2.006307
$\bar{g}_Z$		2.006066
$\bar{A}_X$		15.650 G
$\bar{A}_Y$		14.707 G
$\bar{A}_Z$		16.743 G
$\tau$	0.007 ns	30 ns
Line Width	0.8 G	1.0 G
Fraction	0.55	0.45

**Table 1.** Parameters for simulation of EPR spectra (Fig. 18, 19) of TEMPO radical in DPPC to X and W bands.

## 7. Conclusion

In the conclusion, we presented a uniform approach to EPR spectra analysis based on two-motion model and temperature and viscosity dependence experiment. It was shown to be consistent with molecular dynamics simulations and multifrequency EPR. The present approach is, in principle, applicable to all kinds of spin-labeled macromolecules and polymers. Although TVD is not limited to X-band, this type of spectrometers is most common and especially easy to maintain. At X-band this method may be utilized to full power, as it allows separating rapid motion of spin label and slow Brownian tumbling of macromolecule in solution by simply changing the temperature and viscosity of solvent by adding sucrose. Where it is impossible to carry out such experiment, for example, in membrane structures with embedded spin probe, the two-motion model still remains

applicable, and it is possible to follow the same spectra simulation approach as used in conjunction with temperature and viscosity dependence. The two-motion model for nitroxide spin label dynamics can be applied successfully to interpretation of EPR spectra of most systems involving covalently bound as well as non-bound spin probes (eg, TEMPO radical embedded in membrane). It should be noted, there is one weakness in the proposed method – relatively small (1-4 G) shifts of rather broad peaks has to be measured with sufficient degree of accuracy. Sometimes series of EPR spectra obtained at different conditions may appear very similar, but still they are distinguished by the position of broad outer peaks. With proposed method, it is possible to carry out purposefully the interpretation of EPR spectra of any spin-labeled biological object. Elucidation of microscale dynamical features from its EPR spectra represents an extremely difficult problem. This inverse problem of EPR spectroscopy still has no unequivocal solution. This is partially due to method limitations, but they may be partially overcome by using TVD approach, which extracts additional information from a set of EPR spectra at different conditions. The detailed system dynamics may be obtained from MD simulations and verified against experimental EPR data by using order parameters, as it was shown here on an example of Barstar-Barnase complex formation. The uniform method as described here is, therefore, considered to be a very big step forward for the resolution of the inverse EPR problem for spin-labeled macromolecules and other biological nanoscale objects.

## Author details

Yaroslav Tkachev and Vladimir Timofeev

*V.A. Engelhardt Institute of Molecular Biology/RAS, Moscow, Russia*

## 8. References

- Dudich I.V., Timofeev V.P., Volkenstein M.V., and Misharin A.Yu. (1977) Measurement of rotational correlation time of macromolecules by the ESR method in the case of a covalently bound spin label. *Molecular Biology (translated from Russian)*. 11, 531-538.
- Goldman S.A., Bruno G.V., Freed J.H. (1972). Estimating slow motional rotational correlation times for nitroxides by electron spin resonance. *J. Phys. Chem.* 76, 1858-1860.
- Halle B. (2009). The physical basis of model-free analysis of NMR relaxation data from proteins and complex fluids. *J. Chem. Phys.* 131, 224507-224521.
- Humphrey, W., Dalke, A. and Schulten, K. (1996). "VMD - Visual Molecular Dynamics", *J. Molec. Graphics*, , vol. 14, pp. 33-38.
- Frederick K. K., Sharp K. A., Warischalk N., and Wand A.J. (2008). Re-evaluation of the model-free analysis of fast internal motion in proteins using NMR relaxation, *J. Phys. Chem. B*, 112, 12095–12103.
- Kuznetsov A.N., Wasserman A.M., Volkov A.Yu., Korst N.N. (1971). Determination of rotational correlation time of nitric oxide radicals in a viscous medium. *Chem. Phys. Letters*. 12, 103-106.

- Lipari G., and Szabo A. (1982). Model-free approach to the interpretation of nuclear magnetic resonance relaxation in macromolecules. 1. Theory and range of validity. *J. Am. Chem. Soc.* 104, 4546-4559.
- Mason R., and Freed J.H. (1974). Estimating microsecond rotational correlation times from lifetime broadening of nitroxide ESR spectra near the rigid limit. *J. Phys. Chem.* 78, 1321-1323.
- McCalley R.C., Shimshick E.J., and McConnell H.M. (1972). The effect of slow rotational motion on paramagnetic resonance spectra. *Chem. Phys. Lett.* 13, 115-119.
- Phillips J.C., Rosemary Braun, Wei Wang, James Gumbart, Emad Tajkhorshid, Elizabeth Villa, Christophe Chipot, Robert D. Skeel, Laxmikant Kale, and Klaus Schulten. (2005). Scalable molecular dynamics with NAMD. *Journal of Computational Chemistry*, 26:1781-1802.
- Smirnov A.I., Smirnova T.I., and Morse II P.D. (1995). Very High Frequency Electron Paramagnetic Resonance of 2,2,6,6-Tetramethyl-1-Piperidinyloxy in 1,2-Dipalmitoyl-*sn*-Glycero-3-Phosphatidylcholine Liposomes: Partitioning and Molecular Dynamics. *Biophysical J.* 68, 2350-2360.
- Shimshick E.J., McConnell H.M. (1972). Rotational correlation time of spin-labeled  $\alpha$ -chymotrypsin. *Biochem. Biophys. Res. Commun.* 46, 321-326.
- Shapiro A. B., Volodarskii L. B., Krasochka O. N., Avtomyan L. O., and Rozantsev E. G. (1979). *Dokl. Akad. Nauk. SSSR.* 248, 1135-1139.
- Slichter C.P., (1980). Principles of Magnetic Resonance. Springer-Verlag. Berlin, Heidelberg. New York.
- Stendardo E, Pedone A., Barone V. (2010). Extension of the AMBER force-field for the study of large nitroxides in condensed phases. *Phys Chem Chem Phys.* 12, 11697-709.
- Stone T.J., Buckman T., Nordio P.L., and McConnell H.M. (1965). Spin-labeled biomolecules. *Proc. Nat. Acad. Sci. U.S.* 54, 1010-1017.
- Timofeev V. P. (1986). Segmental mobility of poly(U) and the spin label method. *Molecular Biology (translated from Russian).* 20, 557-568.
- Timofeev V. P., and Samarianov B. A. (1993). About new universal approach to the EPR spectra simulation of the spin-labeled macromolecules. *Appl. Magn. Reson.* 4, 523-539.
- Timofeev V. P., and Samarianov B. A. (1995). Dynamics of macromolecule spin-labeled side chain groups by electron spin resonance spectra simulation. *J. Chem. Soc. PERKIN TRANS. 2,* 2175-2181.
- Timofeev V.P., Novikov V.V., Tkachev Y.V., Balandin T.G., Makarov A.A., Deyev S.M. (2008). Spin label method reveals barnase-barstar interaction: a temperature and viscosity dependence approach. *J. Biomol. Struct. Dyn.* 25, 525-534.
- Tkachev Ya.V., and Timofeev V.P. (2008). Fast Motion Models Help Separating Dynamic Effects on EPR Spectra of Spin-Labeled Macromolecules. *5th International Conference of Nitroxide Radicals*, Ancona , Italy, September 7-11.

Tkachev Ya.V. (2009). The general form of fast oscillation model and its consequences for nitroxide EPR spectra interpretation in biological systems. *EUROMAR Magnetic Resonance Conference*, Gothenburg, Sweden, July 5-9.

Tkachev Ya.V. (2010). Selective modelling of effects of a fast rotational motion nitroxide in EPR spectra of spin-labeled macromolecules. *PhD Thesis Dissertation*. Moscow.

IntechOpen

IntechOpen